

The best of both worlds: combining population genetic and quantitative genetic models

L. Dekens^{*†}, S.P. Otto[‡] and V. Calvez[§]

November 22, 2021

Abstract

Traits under migration-selection balance are increasingly shown to exhibit complex patterns of genetic architecture, with allelic differences of varying magnitude. However, studying the influence of a large number of small allelic effects on the maintenance of spatial polymorphism is mathematically challenging, due to the high complexity of the systems that arise. Here we propose a new methodology that allows us to take into account the combined contributions of a major locus and of a quantitative background resulting from small effect loci, inherited according to the infinitesimal model. In a regime of small variance contributed by the quantitative loci, we found new arguments of convex analysis to justify that traits are concentrated around the major alleles effects according to a normal distribution, which leads to a slow-fast analysis approach. By applying it to a symmetrical two patch model, we predict an undocumented phenomenon of loss of polymorphism at the major locus despite strong selection for local adaptation under some conditions, where the infinitesimal quantitative background slowly disrupts the fast established symmetrical polymorphism at the major locus, which is confirmed by individual-based simulations. We also provide a comprehensive toolbox designed to describe how to apply our method to more complex population genetic models.

Introduction

Many species, if not most, evolve in heterogeneous habitats, where varying selection acts upon phenotypic traits in a manner that causes local adaptation. The genetic architecture that underlies those traits is known to present an array of possibilities, from major responses at one particular gene to diffuse polygenic responses (Slate 2005; Walsh and Lynch 2018). The genetic basis of adaptation has been the subject of an ongoing debate since the early days of evolutionary biology. On the one hand, the field of population genetics explicitly describes and models the dynamics of a few major genes and alleles that have discrete effects, like eye color. On the other hand, the quantitative genetic field explores the evolution of quantitative and continuous traits, like limb size, which are thought to arise from the combined small effects of many genes. A first theoretical milestone in the relationship between the two fields was reached in 1919, when Fisher proposed the infinitesimal model to formalize how such a polygenic trait can be inherited, using the Mendelian framework, clarifying the connection between the two genetic approaches (Fisher 1919). His framework was subsequently made

^{*}Institut Camille Jordan, UMR5208 UCBL/CNRS, Université de Lyon, 69100 Villeurbanne, France.

[†]dekens@math.univ-lyon1.fr

[‡]Department of Zoology, University of British Columbia, Vancouver, BC Canada.

[§]Institut Camille Jordan, UMR5208 UCBL/CNRS, 69100 Villeurbanne, France.

more precise (Bulmer 1971; Lange 1978) and recently justified in various situations using a multi-loci model and a central limit theorem approach (Barton, Etheridge, and Véber 2017).

In the last four decades, enormous progress in genome sequencing has allowed for more data to inform this debate on the genetic architecture underlying traits under selection. However, global conclusions on when a major allele or a polygenic response evolves are still yet to be drawn. For example, as reviewed in Walsh and Lynch (2018), one notable paradox surrounding the study of the evolution of resistance to the insecticide BT toxin is the difference of results between field and lab experiments. Indeed, in the field, major effects are more often found to be the main drivers of evolution of resistance than in the lab, where a polygenic response is more common (McKenzie and Batterham 1994), even if intensity of selection might not differ (Groeters and Tabashnik 2000). Moreover, the length of the experiment seems to matter: the results of QTL mapping on long-term experiments involving crosses between lines subjected to opposing directional selection (like the Illinois corn experiment) often suggest that a polygenic response emerges over time, due to a large number of QTL of small additive effects (see Laurie et al. 2004; Dudley et al. 2007). Note that such a setting of opposing directional selection can arise in heterogeneous environments, where different phenotypic optima are selectively favoured in different patches.

In order to gain general insights on the likely genetic architecture underlying a trait experiencing heterogeneous selection, one should turn to models that analyse population dynamics of a trait resulting from multiple loci with different effect size on the trait, with spatial heterogeneity. In population genetics, one-locus or two-locus models in heterogeneous environments are well studied (Nagylaki and Lou 2001; Bürger and Akerman 2011), with a nuanced picture when including the effect of drift (Yeaman and Otto 2011). A two-deme two-locus model is analysed in Geroldinger and Bürger (2014), which in particular shows that a concentrated genetic architecture (a major locus and a tightly linked minor one) maintains polymorphism (full or single-locus) even under high migration rates when selection acts in opposite directions in the two patches. Increasing the number of loci quickly leads to an analytical complexity too great for a general study. There also exist multi-loci models in heterogeneous environments (Lythgoe 1997; Szép, Sachdeva, and Barton 2021), but they focus on equal allelic effects. On the other end of the spectrum, quantitative genetic models do not typically account for additional discrete allelic effects on the focal quantitative trait (for sexually reproducing populations in heterogeneous environment, see Ronce and Kirkpatrick 2001; Hendry, Day, and Taylor 2001; Dekens 2020).

To our knowledge, the first model that bridges this gap is from Lande (1983). In this work, the author considers the dynamics of a major locus where two alleles segregate along with a polygenic background, in a diploid population subjected to a sudden change of environment. He models the influence of the polygenic background on the trait by assuming that the trait distribution for each genotype at the major effect locus is Gaussian, centered around the phenotype of each genotype at the major effect locus. This study opened the way for more recent work on the genetic architecture of adaptation in a suddenly changing environment, where the central question is whether this adaptation is due to major allelic sweeps or to subtle shifts in the frequency of many small effect alleles. In Chevin and Hospital (2008), the authors extend the framework of Lande (1983) to include less specific selection functions than exponential ones. Subsequent studies (Vladar and Barton 2014; Jain and Stephan 2017) explicitly model the short-term dynamics of a polygenic trait in a mutation-selection balance, following a sudden change of environment. They show that there exists a sharp threshold in allelic sizes under which polymorphism remains and over which fixation occurs. Lately, in a similar context, Höllinger, Pennings, and Hermisson (2019) proposes an extension to take genetic drift

into account on the dynamics of adaptation with a polygenic binary trait under mutation-selection balance. However, all those works from Lande (1983) to Höllinger, Pennings, and Hermisson (2019) study panmictic populations, without spatial structure, even though spatial heterogeneities generate gene flow, which indirectly shapes genetic architecture through local adaptation (see Yeaman and Whitlock (2011), or below for more details). Moreover, they focus solely on the dynamics of the allelic frequencies without considering their coupling with population size dynamics, assuming it to be constant.

The aim of this work is twofold. A first global aim is to propose a hybrid framework between population and quantitative genetics, which allows us to study analytically the long-term eco-evo dynamics of a sexually reproducing population characterized by a composite trait resulting from the interplay between a few major loci and a quantitative polygenic background, in spatially heterogeneous environments (migration-selection balance). We want to emphasize that, by "eco-evo dynamics", we mean that we study both the ecological and evolutionary dynamics of the local trait distributions and therefore do not assume that the sizes of the populations remain constant; rather, they are variables of the system. Furthermore, we aspire to step back from the Gaussian assumption made by Lande (1983) and Chevin and Hospital (2008) to model the background polygenic effect on the trait and propose a framework that does not make a priori assumptions on its shape. Instead, our model relies on an extension of the standard infinitesimal model (Fisher 1919), that encodes both the inheritance of the quantitative background and the major alleles. Analytical progress is possible, despite not specifying the shape of the trait distribution, in a regime of small segregational variance for the quantitative component of the trait. This approximation uses the fact that the variance introduced at each event of reproduction by the quantitative background is small compared to the discrete allelic effects at major loci. This modelling regime allows us to use a methodology developed by Diekmann et al. (2005), inspired by perturbative tools of optic geometrics. This method has been used in several quantitative genetic studies, first for asexually reproducing populations (Perthame and Barles 2008; Barles, Mirrahimi, and Perthame 2009; Mirrahimi 2017; Mirrahimi and Gandon 2020) and more recently models using the infinitesimal model of sexual reproduction (Bouin et al. n.d.; Calvez, Garnier, and Patout 2019; Patout 2020; Dekens 2020).

A second aim is to illustrate the insights given by our framework for local adaptation, by applying it to the simplest case: a haploid population living in a two patch environment, where selection acts on a trait that results from the segregation of two major alleles at a single locus along with a quantitative polygenic background. This choice is partly inspired by the study of Yeaman and Whitlock (2011), which looks at the emergence of patterns in the genetic architecture of local adaptation in a migration-selection balance setting through individual-based simulations. Our model also bridges the following population genetic and quantitative genetic models:

1. The one-locus haploid model in a two-patch environment, which considers two alleles A and a segregating at the same locus, each improving the survival chance in one of the habitats and being deleterious in the other. With symmetrical migration and selection, this model predicts that *polymorphism at the focal locus is always stable*, whenever the metapopulation persists (see Remark 3 and Proposition 3.3 for a proof of this fact). We aim at challenging the robustness of this conclusion by asking: *does this prediction hold when adding a small perturbation due to a quantitative polygenic component on the trait under local selection?*
2. The quantitative genetic model from Dekens (2020), which studies the eco-evo dynamics of a quantitative trait in a heterogeneous environment, where the trait is inherited ac-

cording to the standard version of the infinitesimal model. Our work can be seen as an extension of this model, to which we add the segregation of two major alleles at a single locus. Moreover, if one major allele fixes (loss of polymorphism), the two models are equivalent. Since Dekens (2020) gives a complete analytical description of the outcomes of their system (in the small segregation variance regime), the outcomes for our present study are known given the fixation of a major allele. Therefore, *our study focuses on the description of polymorphism at the major locus and its stability.*

Contributions. We show that our hybrid model gives new analytical insights on the stability of polymorphism at a major locus underlying local adaptation in a symmetrical heterogeneous environment, which is not captured by the one-locus haploid population genetic model. Due to small perturbations induced by the quantitative component of the trait around the genotypic effects of the major alleles, polymorphism at the major locus is lost both at low and high levels of selection, below a certain level of migration. The first region of loss of polymorphism, at low selection intensities, is intuitively expected, as migration blends more strongly than selection differentiates. More surprising is the loss of polymorphism at high intensities of selection, where one would expect polymorphism at the major locus to be strongly favoured. Up to our knowledge, this phenomenon, where quantitative differences displace polymorphism at a major locus, has not yet been documented. We confirm that our analysis is qualitatively consistent with individual-based simulations.

This study-case suggests that the long-term influence of a quantitative polygenic background on a major loci polymorphic equilibrium can lead to unforeseen phenomena. In this work, we present an integrative framework that is meant to help analytically bridge population genetics and quantitative genetics that is meant to help analytically identifying them. Our method goes deeper than previous models (Lande 1983) by justifying in a certain regime of small variance that the traits are normally distributed around the major alleles effects, thanks to new arguments of convex analysis. It allows a slow-fast analysis, that ultimately leads to derive the conditions for when the infinitesimal quantitative background slowly disrupts the fast established symmetrical polymorphism at the major locus.

Furthermore, we provide a comprehensive toolbox that describes how to apply our methodology to more general cases in terms of number of major loci, number of patch, and form of selection for haploid or diploid populations (see Appendices A and B).

Outline. In Section 1, we first present how we build our hybrid model. We detail how we incorporate the effects of selection acting on major alleles segregating at a single locus within a generic quantitative genetic model in a two-patch environment, and their inheritance, thanks an extension to the infinitesimal model. Next, in Section 2, we use a perturbative approach and present new arguments of convex analysis to derive a closed moment-based system in a regime where the segregational variance of the quantitative component of the trait is small compared to the major gene effect. This approach allows us to perform a separation between ecological and evolutionary time scales that leads to an asymptotic system with reduced complexity (Section 3). In Section 4, we analyse the stability of the polymorphism at the major locus (for analytical purposes, we restrict ourselves to the case where the environment is symmetrical in that section). Next in Section 5, we confirm the phenomena of loss of polymorphism at the major locus with individual-based simulations.

1 Model

1.1 From a generic quantitative genetic model to a hybrid model.

We consider a haploid population reproducing sexually and characterized by a quantitative trait ζ in a heterogeneous environment with two habitats connected by constant migration at rate \mathbf{m}_1 (from habitat 1 to habitat 2) and \mathbf{m}_2 (from habitat 2 to habitat 1). Following classical models of quantitative genetics, we model each habitat i selecting toward a different optimum θ_i with strength \mathbf{g}_i . Maladaptation and local uniform competition for resources (with intensity κ_i in deme i) are sources of mortality leading to a per capita decline at rate:

$$-g_i(\zeta - \theta_i)^2 - \kappa_i N_i,$$

for individuals of trait ζ in habitat i (N_i denotes the local population size). At time $t \geq 0$, let $\mathbf{n}_1(t, \zeta)$ and $\mathbf{n}_2(t, \zeta)$ be the local trait densities in patches 1 and 2, and $\mathcal{B}[\mathbf{n}_i](t, \zeta)$ the number of individuals born with a trait ζ in habitat i , with reproduction occurring at rate λ_i . The dynamics of the local trait densities read:

$$\begin{cases} \frac{\partial n_1}{\partial t}(t, \zeta) = \lambda_1 \mathcal{B}[n_1](t, \zeta) - g_1 (\zeta - \theta_1)^2 n_1(t, \zeta) - \kappa_1 N_1(t) n_1(t, \zeta) \\ \quad + m_2 n_2(t, \zeta) - m_1 n_1(t, \zeta), \\ \frac{\partial n_2}{\partial t}(t, \zeta) = \lambda_2 \mathcal{B}[n_2](t, \zeta) - g_2 (\zeta - \theta_2)^2 n_2(t, \zeta) - \kappa_2 N_2(t) n_2(t, \zeta) \\ \quad + m_1 n_1(t, \zeta) - m_2 n_2(t, \zeta). \end{cases} \quad (1)$$

We can define the trait axis such that: $\boldsymbol{\theta} := \boldsymbol{\theta}_2 = -\boldsymbol{\theta}_1 > 0$ without loss of generality. We next describe the novel aspect of this work, which allows the trait $\boldsymbol{\zeta}$ to be sum of two components, a major effect locus and an quantitative background \mathbf{z} . We furthermore describe the sexual reproduction operator used.

Major effect. The first component comes from a locus where two alleles A/a are segregating. They have a major effect on the trait: η_A and η_a . Inheritance of this locus is Mendelian.

Quantitative background. The second component, denoted by $z \in \mathbb{R}$, represents the quantitative background due to infinitesimally small additive contributions to the trait from a large number of unlinked alleles. Although it comes from infinitesimally small contributions, z should not be thought as being necessarily small, due to the large number of alleles contributing to it. We also assume that the major locus is effectively unlinked with the small-effect ones.

Inheritance of the trait: an extension of the infinitesimal model. Let us recall that the infinitesimal model, first introduced in Fisher (1919), provides a way to encode efficiently the inheritance of complex traits coming from a large number of alleles, each with small effects. The classical version states that an offspring receives a trait \mathcal{Z} from its parents with traits \mathcal{Z}_1 and \mathcal{Z}_2 , where \mathcal{Z} differs from the mean parental trait $\frac{\mathcal{Z}_1 + \mathcal{Z}_2}{2}$ following a centered Gaussian law, with variance $\frac{\sigma^2}{2}$. The latter accounts for the stochasticity of segregation, and therefore the variance is called the segregational variance. Specifically:

$$\mathcal{Z}|\mathcal{Z}_1, \mathcal{Z}_2 \sim \frac{\mathcal{Z}_1 + \mathcal{Z}_2}{2} + \mathcal{Y}, \quad \mathcal{Y} \sim \mathcal{N}\left(0, \frac{\sigma^2}{2}\right), \quad \mathcal{Y} \perp \mathcal{Z}_1, \mathcal{Z}_2.$$

The Mendelian view of the infinitesimal model has been discussed in Fisher (1919), Bulmer (1971), and Lange (1978): the common interpretation is that the trait results from a large number of small additive contributions at unlinked loci. For a more in depth description, see Barton, Etheridge, and Véber (2017).

Because the trait we are considering is a composite of a major effect locus inherited according to Mendelian laws and an infinitesimal background, it is natural to use an extension of the infinitesimal model for this hybrid case. Now, the offspring's trait $(\mathcal{A}, \mathcal{Z})$ given their parents $(\mathcal{A}_1, \mathcal{Z}_1)$ and $(\mathcal{A}_2, \mathcal{Z}_2)$ reads:

$$(\mathcal{A}, \mathcal{Z},) \mid (\mathcal{A}_1, \mathcal{Z}_1), (\mathcal{A}_2, \mathcal{Z}_2) \sim \left(X\mathcal{A}_1 + (1 - X)\mathcal{A}_2, \frac{\mathcal{Z}_1 + \mathcal{Z}_2}{2} + \mathcal{Y} \right), \quad (2)$$

where $\mathcal{Y} \sim \mathcal{N}\left(0, \frac{\sigma^2}{2}\right)$ follows a centered Gaussian law of variance $\frac{\sigma^2}{2}$ and $X \sim B\left(\frac{1}{2}\right)$ follows a Bernoulli law with parameter $\frac{1}{2}$ (assuming fair meiosis). The latter are independent of each other and of $\mathcal{Z}_1, \mathcal{Z}_2, \mathcal{A}_1, \mathcal{A}_2$.

1.2 Modified reproduction operator.

Let us translate Eq. (2) into a continuous density model. Let $\mathbf{n}_i^A(\mathbf{z})$ (respectively $\mathbf{n}_i^a(\mathbf{z})$) denote the density of individuals of patch i carrying allele A (respectively a) along with an infinitesimal background \mathbf{z} , therefore having a trait $\boldsymbol{\zeta} = \boldsymbol{\eta}^A + \mathbf{z}$ (respectively, $\boldsymbol{\eta}^a + \mathbf{z}$). In agreement with Eq. (2), the number of offspring born with the allele A and an infinitesimal contribution \mathbf{z} in habitat i then reads:

$$\begin{aligned} \mathcal{B}_\sigma^A[\mathbf{n}_i^A, \mathbf{n}_i^a](\mathbf{z}) &= \int_{\mathbb{R}^2} \frac{1}{\sqrt{\pi}\sigma} \exp \left[-\frac{\left(\mathbf{z} - \frac{\mathbf{z}_1 + \mathbf{z}_2}{2}\right)^2}{\sigma^2} \right] \times \\ &\quad \frac{1}{N_i} \left[\mathbf{n}_i^A(\mathbf{z}_1) \mathbf{n}_i^A(\mathbf{z}_2) + \frac{1}{2} \left[\mathbf{n}_i^A(\mathbf{z}_1) \mathbf{n}_i^a(\mathbf{z}_2) + \mathbf{n}_i^a(\mathbf{z}_1) \mathbf{n}_i^A(\mathbf{z}_2) \right] \right] d\mathbf{z}_1 d\mathbf{z}_2 \\ &= \int_{\mathbb{R}^2} \frac{1}{\sqrt{\pi}\sigma} \exp \left[-\frac{\left(\mathbf{z} - \frac{\mathbf{z}_1 + \mathbf{z}_2}{2}\right)^2}{\sigma^2} \right] \mathbf{n}_i^A(\mathbf{z}_1) \frac{\mathbf{n}_i^A(\mathbf{z}_2) + \mathbf{n}_i^a(\mathbf{z}_2)}{N_i} d\mathbf{z}_1 d\mathbf{z}_2. \end{aligned}$$

Similarly, the corresponding number of offspring born with the allele a and an infinitesimal part \mathbf{z} reads:

$$\begin{aligned} \mathcal{B}_\sigma^a[\mathbf{n}_i^A, \mathbf{n}_i^a](\mathbf{z}) &= \int_{\mathbb{R}^2} \frac{1}{\sqrt{\pi}\sigma} \exp \left[-\frac{\left(\mathbf{z} - \frac{\mathbf{z}_1 + \mathbf{z}_2}{2}\right)^2}{\sigma^2} \right] \times \\ &\quad \frac{1}{N_i} \left[\mathbf{n}_i^a(\mathbf{z}_1) \mathbf{n}_i^a(\mathbf{z}_2) + \frac{1}{2} \left[\mathbf{n}_i^A(\mathbf{z}_1) \mathbf{n}_i^a(\mathbf{z}_2) + \mathbf{n}_i^a(\mathbf{z}_1) \mathbf{n}_i^A(\mathbf{z}_2) \right] \right] d\mathbf{z}_1 d\mathbf{z}_2 \\ &= \int_{\mathbb{R}^2} \frac{1}{\sqrt{\pi}\sigma} \exp \left[-\frac{\left(\mathbf{z} - \frac{\mathbf{z}_1 + \mathbf{z}_2}{2}\right)^2}{\sigma^2} \right] \mathbf{n}_i^a(\mathbf{z}_1) \frac{\mathbf{n}_i^a(\mathbf{z}_2) + \mathbf{n}_i^A(\mathbf{z}_2)}{N_i} d\mathbf{z}_1 d\mathbf{z}_2. \end{aligned}$$

The operator reproduction \mathcal{B}_σ indicates that it is more relevant to model the dynamics of the two local allelic densities $\mathbf{n}_i^a, \mathbf{n}_i^A$, instead of \mathbf{n}_i (which is their sum). From now on, we will therefore adopt this point of view.

1.3 Dimensionless system

Let us rescale Eq. (1) according to:

$$\eta^A := \frac{\eta^A}{\theta}, \quad z := \frac{z}{\theta}, \quad g_i := \frac{g_i \theta^2}{\lambda_1}, \quad m_i := \frac{m_i}{\lambda_1}, \quad \varepsilon := \frac{\sigma}{\theta}, \quad t := \varepsilon^2 \lambda_1 t, \quad \alpha := \frac{\kappa_1}{\kappa_2}, \quad \lambda := \frac{\lambda_2}{\lambda_1},$$

and introduce the rescaled trait densities:

$$n_{\varepsilon,i}^A(t, z) := \frac{\kappa_i}{\lambda_1} n_i^A(t, z), \quad n_{\varepsilon,i}^a(t, z) := \frac{\kappa_i}{\lambda_1} n_i^a(t, z).$$

so that Eq. (1) reads:

$$\left\{ \begin{array}{l} \varepsilon^2 \frac{\partial n_{\varepsilon,1}^A}{\partial t}(t, z) = \mathcal{B}_\varepsilon^A(n_{\varepsilon,1}^A, n_{\varepsilon,1}^a)(t, z) - g_1(z + \eta^A + 1)^2 n_{\varepsilon,1}^A(t, z) - N_{\varepsilon,1}(t) n_{\varepsilon,1}^A(t, z) \\ \quad + \alpha m_2 n_{\varepsilon,2}^A(t, z) - m_1 n_{\varepsilon,1}^A(t, z), \\ \varepsilon^2 \frac{\partial n_{\varepsilon,1}^a}{\partial t}(t, z) = \mathcal{B}_\varepsilon^a(n_{\varepsilon,1}^a, n_{\varepsilon,1}^A)(t, z) - g_1(z + \eta^a + 1)^2 n_{\varepsilon,1}^a(t, z) - N_{\varepsilon,1}(t) n_{\varepsilon,1}^a(t, z) \\ \quad + \alpha m_2 n_{\varepsilon,2}^a(t, z) - m_1 n_{\varepsilon,1}^a(t, z), \\ \varepsilon^2 \frac{\partial n_{\varepsilon,2}^A}{\partial t}(t, z) = \lambda \mathcal{B}_\varepsilon^A(n_{\varepsilon,2}^A, n_{\varepsilon,2}^a)(t, z) - g_2(z + \eta^A - 1)^2 n_{\varepsilon,2}^A(t, z) - N_{\varepsilon,2}(t) n_{\varepsilon,2}^A(t, z) \\ \quad + \frac{m_1}{\alpha} n_{\varepsilon,1}^A(t, z) - m_2 n_{\varepsilon,2}^A(t, z), \\ \varepsilon^2 \frac{\partial n_{\varepsilon,2}^a}{\partial t}(t, z) = \lambda \mathcal{B}_\varepsilon^a(n_{\varepsilon,2}^a, n_{\varepsilon,2}^A)(t, z) - g_2(z + \eta^a - 1)^2 n_{\varepsilon,2}^a(t, z) - N_{\varepsilon,2}(t) n_{\varepsilon,2}^a(t, z) \\ \quad + \frac{m_1}{\alpha} n_{\varepsilon,1}^a(t, z) - m_2 n_{\varepsilon,2}^a(t, z), \end{array} \right. \quad (3)$$

where the rescaled reproduction operator is given by:

$$\mathcal{B}_\varepsilon^A(n_{\varepsilon,i}^A, n_{\varepsilon,i}^a)(t, z) = \frac{1}{\sqrt{\pi}\varepsilon} \int_{\mathbb{R}^2} \exp \left[\frac{-(z - \frac{z_1+z_2}{2})^2}{\varepsilon^2} \right] n_{\varepsilon,i}^A(t, z_1) \frac{n_{\varepsilon,i}^A(t, z_2) + n_{\varepsilon,i}^a(t, z_2)}{N_{\varepsilon,i}(t)} dz_1 dz_2. \quad (4)$$

Working assumption 1. *One can notice that if one allele, for instance A, has fixed and the other is lost ($n^a(z) = 0$), then \mathcal{B}_σ^A coincides with the infinitesimal model reproduction operator used in Dekens (2020). Therefore, in that case, then (3) is the same system as the one fully analysed in Dekens (2020), up to a translation: $z + \eta^A \rightarrow \tilde{z}$. Hence, in all that follows, we assume that both alleles are still present in the population and focus on the conditions of the persistence of this polymorphism.*

2 Derivation of a moment-based system in the regime of small variance: $\varepsilon^2 \ll 1$

2.1 The regime of small variance: a formal analysis.

Presentation of the methodology. We choose to place our study in a regime where the amount of diversity introduced by the segregation of the infinitesimal background at each event of reproduction is small in comparison to the difference between the habitats' optima, which reads:

$$\frac{\sigma^2}{\theta^2} \ll 1 \implies \varepsilon^2 \ll 1.$$

In this regime of small variance, the trait distributions are expected in the limit to be Dirac masses centred at the major locus genotypes, where our focus is to determine the distribution near this limit. Diekmann et al. (2005) introduced in 2005 a methodology to determine the dynamics of the trait values at which the distribution gets concentrated. This methodology has since been used successfully to study several evolutionary questions, initially for asexual models where the diversity generated by mutations is modelled by a linear operator translating the distribution of mutational effects (Perthame and Barles 2008; Barles, Mirrahimi, and Perthame 2009; Mirrahimi 2017; Mirrahimi and Gandon 2020), and recently adapted to study sexually reproducing populations with the infinitesimal model operator (Bouin et al. n.d.; Calvez, Garnier, and Patout 2019; Patout 2020; Dekens 2020). The method consists in defining proxies U_ε from the trait densities n_ε through a suitable transformation so that such proxies are regular functions (by comparison to Dirac masses) and their asymptotic analysis is easier. Studying them often induces a reduction in the complexity of the system and retain fundamental quantitative information about the distributions, such as around which traits they are centred. Here, we follow quantitative genetic studies that use the infinitesimal model according to the same methodology (Bouin et al. n.d.; Calvez, Garnier, and Patout 2019; Patout 2020; Dekens 2020) and define the proxies $U_{\varepsilon,i}^A$ (resp. $U_{\varepsilon,i}^a$):

$$n_{\varepsilon,i}^A = \frac{1}{\sqrt{2\pi\varepsilon}} e^{-\frac{U_{\varepsilon,i}^A}{\varepsilon^2}}, \quad n_{\varepsilon,i}^a = \frac{1}{\sqrt{2\pi\varepsilon}} e^{-\frac{U_{\varepsilon,i}^a}{\varepsilon^2}}. \quad (5)$$

Figure 1 displays an example of this kind of exponential transformation (called Hopf-Cole transformation in scalar conservation laws). A key observation is that the trait density n_ε concentrates at the minima (zero) of U_ε . As the proxies U_ε^A and U_ε^a are expected to be more regular in the regime of small variance, they are thought to be the right object on which to perform a Taylor expansion series to gain information on the asymptotic distributions in the limit of small variance (see Calvez, Garnier, and Patout 2019). We therefore define $u_{0,i}^A$ (resp. $u_{0,i}^a$) as the leading term in the Taylor expansion of $U_{\varepsilon,i}^A$ (resp. $U_{\varepsilon,i}^a$):

$$U_{\varepsilon,i}^A = u_{0,i}^A + \varepsilon^2 u_{1,i}^A + \varepsilon^4 v_{\varepsilon,i}^A, \quad U_{\varepsilon,i}^a = u_{0,i}^a + \varepsilon^2 u_{1,i}^a + \varepsilon^4 v_{\varepsilon,i}^a \quad (6)$$

where $u_{1,i}^A$ and $u_{1,i}^a$ are the next term in the Taylor expansion, and $\varepsilon^4 v_{\varepsilon,i}^A$ and $\varepsilon^4 v_{\varepsilon,i}^a$ are the residues. Calvez, Garnier, and Patout (2019) provides the tools to control these residues and thus rigorously justify that (6) is an admissible Taylor expansion; adapting them is left for future work.

Characterization of the main terms $u_{0,i}^A$ and $u_{0,i}^a$. The first step for the analysis in the regime of small variance is the characterization of the main terms $u_{0,i}^A$ and $u_{0,i}^a$. However, the arguments given in Bouin et al. (n.d.) and used in Dekens (2020) are not sufficient, due to the mixing of alleles and the discrete nature of Mendelian inheritance. However, we extend the convex analysis to circumvent this limitation (Proposition 2.1). Assuming (6) is an admissible Taylor expansion (which is suggested by the analysis of Calvez, Garnier, and Patout (2019)), this step is crucial as it justifies the following formal approximations for $n_{\varepsilon,i}^A$ and $n_{\varepsilon,i}^a$ ($i \in \{1, 2\}$):

$$n_{\varepsilon,i}^A(z) = \frac{e^{-\frac{-(z-z_i)^2}{2\varepsilon^2}}}{\sqrt{2\pi\varepsilon}} e^{-u_{1,i}^A(z) + \mathcal{O}(\varepsilon^2)}, \quad n_{\varepsilon,i}^a(z) = \frac{e^{-\frac{-(z-z_i)^2}{2\varepsilon^2}}}{\sqrt{2\pi\varepsilon}} e^{-u_{1,i}^a(z) + \mathcal{O}(\varepsilon^2)}. \quad (7)$$

Hence, to the leading order, $n_{\varepsilon,i}^A$ and $n_{\varepsilon,i}^a$ are formally Gaussian, centered at the same infinitesimal contribution z_i , with the same variance ε^2 , but they differ in their prefactors, which are

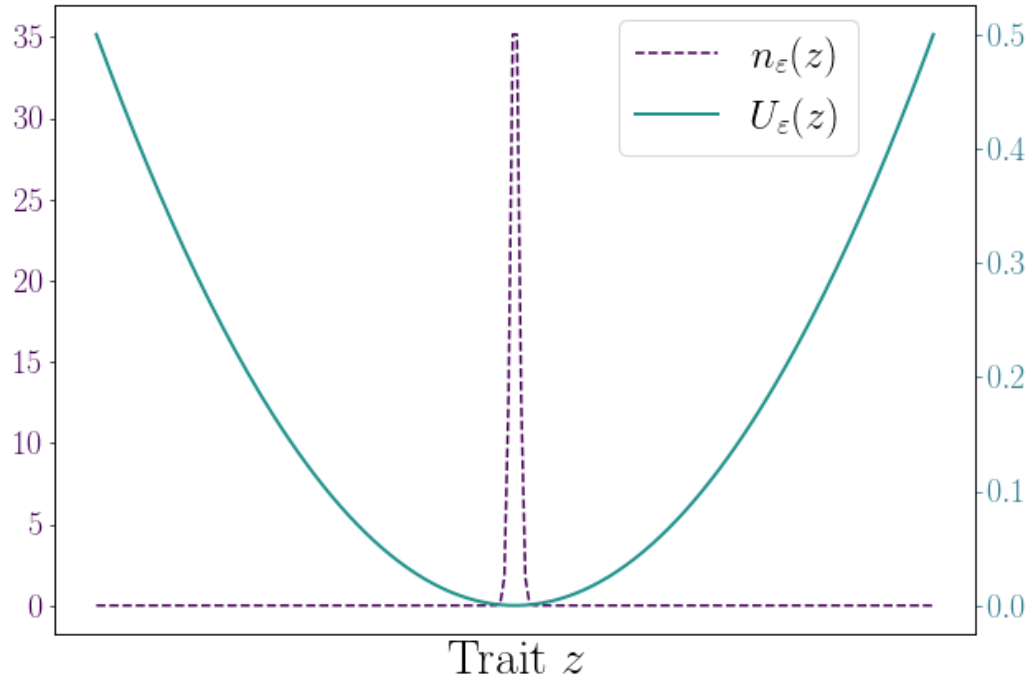


Figure 1: **Illustration of the Hopf-Cole transform to study concentration phenomena.** This transformation unfolds singular distributions n_ε close to a Dirac mass (in purple), by defining more regular proxies: U_ε (in green) such that $n_\varepsilon = \frac{1}{\sqrt{2\pi\varepsilon}}e^{-\frac{U_\varepsilon}{\varepsilon^2}}$. This figure suggests that, when ε vanishes, the limit U is regular and positive and cancels at the support of the limit measure n .

related to the first corrector terms $u_{1,i}^A$ and $u_{1,i}^a$, which generates asymmetries in the distributions.

Remark 1. *The expressions for $n_{\varepsilon,i}^A$ and $n_{\varepsilon,i}^a$ imply that in the regime of small variance, when both alleles A and a are still present in the population, the trait divergence within a habitat is mainly due to the major-effect locus.*

To support (7), we first derive constraints (C) on the main terms $u_{0,i}^A$ and $u_{0,i}^a$. In order for the contribution of both reproduction operators $\mathcal{B}_\varepsilon^A$ and $\mathcal{B}_\varepsilon^a$ to remain well-balanced with the other biological phenomena in the regime of small variance in (3), $u_{0,i}^A$ and $u_{0,i}^a$ formally need to satisfy the following (see Appendix C for the details):

$$\left\{ \begin{array}{l} \forall z \in \mathbb{R}, \quad \max \left[\sup_{z_1, z_2} u_{0,i}^A(z) - \left(z - \frac{z_1 + z_2}{2} \right)^2 - u_{0,i}^A(z_1) - u_{0,i}^A(z_2), \right. \\ \qquad \qquad \qquad \left. \sup_{z_1, z_2} u_{0,i}^A(z) - \left(z - \frac{z_1 + z_2}{2} \right)^2 - u_{0,i}^A(z_1) - u_{0,i}^a(z_2) \right] = 0, \\ \forall z \in \mathbb{R}, \quad \max \left[\sup_{z_1, z_2} u_{0,i}^a(z) - \left(z - \frac{z_1 + z_2}{2} \right)^2 - u_{0,i}^a(z_1) - u_{0,i}^a(z_2), \right. \\ \qquad \qquad \qquad \left. \sup_{z_1, z_2} u_{0,i}^a(z) - \left(z - \frac{z_1 + z_2}{2} \right)^2 - u_{0,i}^A(z_1) - u_{0,i}^a(z_2) \right] = 0. \end{array} \right. \quad (\text{C})$$

Proposition 2.1. *Let u_0^A and u_0^a satisfying Eq. (C), positive almost everywhere and cancelling somewhere. Then, there exists $z^* \in \mathbb{R}$ such that:*

$$\forall z \in \mathbb{R}, \quad u_0^A(z) = u_0^a(z) = \frac{(z - z^*)^2}{2}. \quad (8)$$

The conditions on $u_{0,i}^A$ and $u_{0,i}^a$ in Proposition 2.1 (positive everywhere and cancelling somewhere) are explained in Appendix C.

Consequently, assuming that (6) is the correct ansatz so that we can control the residues in (7) (which the analysis of Calvez, Garnier, and Patout (2019) suggests and provides a framework to show), using the result of Proposition 2.1 in (5) and (6) leads to (7).

Proof. The proof relies on the same kind of approach as in Bouin et al. (n.d.), in which the authors find the solutions to a constraint that is equivalent to (C) with the additional constraint of $u_0^A = u_0^a$. As we do not assume the latter, this proof presents a novel part located in the 4th and 5th points.

1) u_0^A and u_0^a are continuous and have right and left derivatives everywhere. For $z \in \mathbb{R}$, we have:

$$u_0^A(z) - z^2 = \inf_{z_1, z_2} \left[-z \frac{(z_1 + z_2)}{2} + \left(\frac{z_1 + z_2}{2} \right)^2 + u_0^A(z_1) + \min(u_0^A(z_2), u_0^a(z_2)) \right]. \quad (9)$$

Therefore, $z \mapsto u_0^A(z) - z^2$ is concave as infimum of affine functions, and thus continuous and has right and left derivatives. The same holds for $u_0^a - z^2$.

2) u_0^A and u_0^a both cancels only once, and their zeros are the same. First let us show that u_0^A cancels only once. Suppose that $z_1^A \leq z_2^A$ are such that $u_0^A(z_1^A) = u_0^A(z_2^A) = 0$. Then, applying the first constraint to $z = \frac{z_1^A + z_2^A}{2}$ and $u_0^A(z_1) = u_0^A(z_1^A), u_0^A(z_2) = u_0^A(z_2^A)$ leads to:

$$u_0^A \left(\frac{z_1^A + z_2^A}{2} \right) \leq 0.$$

Since u_0^A is non-negative, $\frac{z_1^A + z_2^A}{2}$ is also a zero of u_0^A . We just showed that the midpoint between two zeros of u_0^A is also a zero of u_0^A . Since u_0^A is continuous, by density, it both cancels on $[z_1^A, z_2^A]$. As u_0^A is positive almost everywhere, it cannot cancel on an interval of positive measure, so we deduce that $z_1^A = z_2^A$. The same argument holds for u_0^a , so there exists (z^A, z^a) such that $u_0^A(z^A) = 0$ and $u_0^a(z^a) = 0$.

Let us now show that $z^A = z^a$. Applying the same arguments as before, but on $z = \frac{z^A + z^a}{2}$ and $u_0^A(z_1) = u_0^A(z^A), u_0^a(z_2) = u_0^a(z^a)$ (using the second line of the first equality of (C)), we obtain that $z = \frac{z^A + z^a}{2}$ is also a zero of u_0^A ; Since we showed before that u_0^A cancels only in z^A , we obtain that

$$z^A = z^a =: z^*.$$

3) Convex Legendre conjugates $\hat{u}_0^A(y) = \sup_z (z - z^*)y - u^A(z)$ and $\hat{u}_0^a(y) = \sup_z (z - z^*)y - u^a(z)$. Let us show that:

$$\begin{aligned} \hat{u}_0^A(y) &= \max \left[\frac{y^2}{4} + 2\hat{u}_0^A\left(\frac{y}{2}\right), \frac{y^2}{4} + \hat{u}_0^A\left(\frac{y}{2}\right) + \hat{u}_0^a\left(\frac{y}{2}\right) \right], \\ \hat{u}_0^a(y) &= \max \left[\frac{y^2}{4} + 2\hat{u}_0^a\left(\frac{y}{2}\right), \frac{y^2}{4} + \hat{u}_0^a\left(\frac{y}{2}\right) + \hat{u}_0^A\left(\frac{y}{2}\right) \right]. \end{aligned} \quad (10)$$

Using (9) and commuting the sup, we obtain, for $y \in \mathbb{R}$,

$$\begin{aligned} \hat{u}_0^A(y) &= \sup_z \left[(z - z^*)y - \inf_{z_1, z_2} \left(\left(z - \frac{z_1 + z_2}{2} \right)^2 + u_0^A(z_1) + \min(u_0^A(z_2), u_0^a(z_2)) \right) \right] \\ &= \max \left[\sup_{z_1, z_2} \left(-u_0^A(z_1) - u_0^A(z_2) + \sup_z (z - z^*)y - \left(z - \frac{z_1 + z_2}{2} \right)^2 \right), \right. \\ &\quad \left. \sup_{z_1, z_2} \left(-u_0^A(z_1) - u_0^a(z_2) + \sup_z (z - z^*)y - \left(z - \frac{z_1 + z_2}{2} \right)^2 \right) \right]. \end{aligned} \quad (11)$$

Moreover, a straight-forward calculus leads to

$$\begin{aligned} \sup_z (z - z^*)y - \left(z - \frac{z_1 + z_2}{2} \right)^2 &= -\frac{y^2}{4} + y \left(\frac{y + z_1 + z_2}{2} - z^* \right) \\ &= \frac{y^2}{4} + (z_1 - z^*) \frac{y}{2} + (z_2 - z^*) \frac{y}{2}. \end{aligned} \quad (12)$$

Combining (12) and (11) (the fact that $z^A = z^a = z^*$ plays a crucial part for the crossed term) leads to (10).

4) Conservation of order with half arguments. Let us consider $y \in \mathbb{R}$ such that $\hat{u}_0^A(y) \geq \hat{u}_0^a(y)$. Then (10) implies:

$$\max \left[2\hat{u}_0^A\left(\frac{y}{2}\right), \hat{u}_0^A\left(\frac{y}{2}\right) + \hat{u}_0^a\left(\frac{y}{2}\right) \right] \geq \max \left[\hat{u}_0^A\left(\frac{y}{2}\right) + \hat{u}_0^a\left(\frac{y}{2}\right), 2\hat{u}_0^a\left(\frac{y}{2}\right) \right],$$

which in turn implies that

$$\hat{u}_0^A\left(\frac{y}{2}\right) \geq \hat{u}_0^a\left(\frac{y}{2}\right).$$

By recursion, for $k \in \mathbb{N}$, we deduce that

$$\hat{u}_0^A\left(\frac{y}{2^k}\right) \geq \hat{u}_0^a\left(\frac{y}{2^k}\right).$$

5) Showing that $\hat{u}_0^A = \hat{u}_0^a$. Let us still consider $y \in \mathbb{R}$ such that $\hat{u}_0^A(y) \geq \hat{u}_0^a(y)$. Using (13) in (10) leads to

$$\begin{aligned}\hat{u}_0^A\left(\frac{y}{2^k}\right) &= \frac{y^2}{2^{2k+2}} + 2\hat{u}_0^A\left(\frac{y}{2^{k+1}}\right), \\ \hat{u}_0^a\left(\frac{y}{2^k}\right) &= \frac{y^2}{2^{2k+2}} + \hat{u}_0^A\left(\frac{y}{2^{k+1}}\right) + \hat{u}_0^a\left(\frac{y}{2^{k+1}}\right).\end{aligned}\tag{13}$$

The second line implies that

$$\forall k \in \mathbb{N}, \quad \hat{u}_0^a\left(\frac{y}{2^k}\right) - \hat{u}_0^A\left(\frac{y}{2^k}\right) = \hat{u}_0^a\left(\frac{y}{2^{k+1}}\right) - \hat{u}_0^A\left(\frac{y}{2^{k+1}}\right).$$

By continuity of \hat{u}_0^A and \hat{u}_0^a , we obtain

$$\hat{u}_0^A(y) - \hat{u}_0^a(y) = \hat{u}_0^A(z^*) - \hat{u}_0^a(z^*) = 0.$$

As the same can be applied to $y \in \mathbb{R}$ such that $\hat{u}_0^A(y) \leq \hat{u}_0^a(y)$, we obtain

$$\hat{u}_0^A = \hat{u}_0^a.$$

So from now on, we will only show the arguments for \hat{u}_0^A .

6) Computing \hat{u}_0^A . As \hat{u}_0^A is convex by definition, it is continuous and admits left and right derivatives everywhere. Moreover, \hat{u}_0^A has a minimum in 0 and $\hat{u}_0^A(0) = -u_0^A(z^*) = 0$. Therefore (10) implies by recursion (denoting $\alpha := \hat{u}_0^{A'}(0^-)$ and $\beta = \hat{u}_0^{A'}(0^+)$):

$$\forall y > 0 \quad (\text{resp. } < 0), \quad \hat{u}_0^A(y) = \frac{y^2}{2} + \beta y \quad (\text{resp. } \alpha y).\tag{14}$$

Note that 0 being a minimum of \hat{u}_0^A implies that: $\alpha \leq 0 \leq \beta$.

7) Using the convex bi-conjugate to obtain: $u_0^A = \frac{z-z^*}{2}$. We can compute the bi-conjugate's expression from (14):

$$\hat{u}_0^A : z \mapsto \begin{cases} \frac{(z-z^*-\alpha)^2}{2} & \text{if } z < z^* + \alpha \\ 0 & \text{if } z^* + \alpha \leq z \leq z^* + \beta \\ \frac{(z-z^*-\beta)^2}{2} & \text{if } z > z^* + \beta. \end{cases}\tag{15}$$

Standard convexity analysis states also that \hat{u}_0^A is the lower convex envelope of u_0^A .

The first implication is that u_0^A and \hat{u}_0^A coincide on $\mathbb{R} \setminus [z^* + \alpha, z^* + \beta]$, because \hat{u}_0^A is strictly convex there.

The second implication is that $u_0^A(z^* + \alpha) = \hat{u}_0^A(z^* + \alpha) = 0$ (resp. $z^* + \beta$), since $z^* + \alpha$ (resp. $z^* + \beta$) is an extremal point of the graph of \hat{u}_0^A . As any midpoint between two zeros of u_0^A is still a zero of u_0^A (second point of the proof), by density and continuity of u_0^A , u_0^A vanishes on $[z^* + \alpha, z^* + \beta]$. So

$$u_0^A = \hat{u}_0^A.$$

Finally, u_0^A vanishes only at z^* (second point of the proof), so $\alpha = \beta = 0$ and we obtain the desired result. \square

2.2 Moment-based system in the regime of small variance

First, let us derive a formal expansion of the first moments of $n_{\varepsilon,i}^A$ and $n_{\varepsilon,i}^a$ when $\varepsilon^2 \ll 1$ (similar to the derivation in Dekens 2020):

$$\left\{ \begin{aligned} N_{\varepsilon,i}^A &:= \int_{\mathbb{R}} n_{\varepsilon,i}^A(z) dz &&= e^{-u_{1,i}^A(z_i)} \left[1 + \varepsilon^2 \left(\frac{(\partial_z u_{1,i}^A(z_i))^2}{2} - \frac{\partial_z z u_{1,i}^A(z_i)}{2} - v_{i,\varepsilon}^A(z_i) \right) \right] + \mathcal{O}(\varepsilon^4), \\ \overline{z_{\varepsilon,i}^A} &:= \int_{\mathbb{R}} z \frac{n_{\varepsilon,i}^A(z)}{N_{\varepsilon,i}^A} dz &&= z_i - \varepsilon^2 \partial_z u_{1,i}^A(z_i) + \mathcal{O}(\varepsilon^4), \\ (\sigma_{\varepsilon,i}^A)^2 &:= \int_{\mathbb{R}} (z - \overline{z_{\varepsilon,i}^A})^2 \frac{n_{\varepsilon,i}^A(z)}{N_{\varepsilon,i}^A} dz &&= \varepsilon^2 + \mathcal{O}(\varepsilon^4), \\ (\psi_{\varepsilon,i}^A)^3 &:= \int_{\mathbb{R}} (z - \overline{z_{\varepsilon,i}^A})^3 \frac{n_{\varepsilon,i}^A(z)}{N_{\varepsilon,i}^A} dz &&= \mathcal{O}(\varepsilon^4). \end{aligned} \right. \quad (16)$$

Hence, by integration in the regime of small variance, we can close the infinite system of moments derived from (3), producing a system of eight ODEs:

$$\left\{ \begin{aligned} \varepsilon^2 \frac{dN_{\varepsilon,1}^a}{dt} &= N_{\varepsilon,1}^a - \left(N_{\varepsilon,1}^A + N_{\varepsilon,1}^a \right) N_{\varepsilon,1}^a - g_1 \left[\overline{z_{\varepsilon,1}^a} + \eta^a + 1 \right]^2 N_{\varepsilon,1}^a + \alpha m_2 N_{\varepsilon,2}^a - m_1 N_{\varepsilon,1}^a, \\ &\quad + \mathcal{O}(\varepsilon^2), \\ \varepsilon^2 \frac{dN_{\varepsilon,1}^A}{dt} &= N_{\varepsilon,1}^A - \left(N_{\varepsilon,1}^A + N_{\varepsilon,1}^a \right) N_{\varepsilon,1}^A - g_1 \left[\overline{z_{\varepsilon,1}^A} + \eta^A + 1 \right]^2 N_{\varepsilon,1}^A + \alpha m_2 N_{\varepsilon,2}^A - m_1 N_{\varepsilon,1}^A, \\ &\quad + \mathcal{O}(\varepsilon^2), \\ \varepsilon^2 \frac{dN_{\varepsilon,2}^a}{dt} &= \lambda N_{\varepsilon,2}^a - \left(N_{\varepsilon,2}^A + N_{\varepsilon,2}^a \right) N_{\varepsilon,2}^a - g_2 \left[\overline{z_{\varepsilon,2}^a} + \eta^a - 1 \right]^2 N_{\varepsilon,2}^a + \frac{m_1}{\alpha} N_{\varepsilon,1}^a - m_2 N_{\varepsilon,2}^a, \\ &\quad + \mathcal{O}(\varepsilon^2), \\ \varepsilon^2 \frac{dN_{\varepsilon,2}^A}{dt} &= \lambda N_{\varepsilon,2}^A - \left(N_{\varepsilon,2}^A + N_{\varepsilon,2}^a \right) N_{\varepsilon,2}^A - g_2 \left[\overline{z_{\varepsilon,2}^A} + \eta^A - 1 \right]^2 N_{\varepsilon,2}^A + \frac{m_1}{\alpha} N_{\varepsilon,1}^A - m_2 N_{\varepsilon,2}^A, \\ &\quad + \mathcal{O}(\varepsilon^2), \\ \varepsilon^2 \frac{d\overline{z_{\varepsilon,1}^a}}{dt} &= \varepsilon^2 2g_1 \left[-1 - \eta^a - \overline{z_{\varepsilon,1}^a} \right] + \left(\frac{\overline{z_{\varepsilon,1}^A} - \overline{z_{\varepsilon,1}^a}}{2} \right) \frac{N_{\varepsilon,1}^A}{N_{\varepsilon,1}^a} + \alpha m_2 \frac{N_{\varepsilon,2}^a}{N_{\varepsilon,1}^a} \left(\overline{z_{\varepsilon,2}^a} - \overline{z_{\varepsilon,1}^a} \right) + \mathcal{O}(\varepsilon^4), \\ \varepsilon^2 \frac{d\overline{z_{\varepsilon,1}^A}}{dt} &= \varepsilon^2 2g_1 \left[-1 - \eta^A - \overline{z_{\varepsilon,1}^A} \right] + \left(\frac{\overline{z_{\varepsilon,1}^a} - \overline{z_{\varepsilon,1}^A}}{2} \right) \frac{N_{\varepsilon,1}^a}{N_{\varepsilon,1}^A} + \alpha m_2 \frac{N_{\varepsilon,2}^A}{N_{\varepsilon,1}^A} \left(\overline{z_{\varepsilon,2}^A} - \overline{z_{\varepsilon,1}^A} \right) + \mathcal{O}(\varepsilon^4), \\ \varepsilon^2 \frac{d\overline{z_{\varepsilon,2}^a}}{dt} &= \varepsilon^2 2g_2 \left[1 - \eta^a - \overline{z_{\varepsilon,2}^a} \right] + \left(\frac{\overline{z_{\varepsilon,2}^A} - \overline{z_{\varepsilon,2}^a}}{2} \right) \frac{N_{\varepsilon,2}^A}{N_{\varepsilon,2}^a} + \frac{m_1}{\alpha} \frac{N_{\varepsilon,1}^a}{N_{\varepsilon,2}^a} \left(\overline{z_{\varepsilon,1}^a} - \overline{z_{\varepsilon,2}^a} \right) + \mathcal{O}(\varepsilon^4), \\ \varepsilon^2 \frac{d\overline{z_{\varepsilon,2}^A}}{dt} &= \varepsilon^2 2g_2 \left[1 - \eta^A - \overline{z_{\varepsilon,2}^A} \right] + \left(\frac{\overline{z_{\varepsilon,2}^a} - \overline{z_{\varepsilon,2}^A}}{2} \right) \frac{N_{\varepsilon,2}^a}{N_{\varepsilon,2}^A} + \frac{m_1}{\alpha} \frac{N_{\varepsilon,1}^A}{N_{\varepsilon,2}^A} \left(\overline{z_{\varepsilon,1}^A} - \overline{z_{\varepsilon,2}^A} \right) + \mathcal{O}(\varepsilon^4). \end{aligned} \right. \quad (17)$$

Remark 2. As in the analogous ODE system obtained without the major effect locus Dekens (2020), when $\varepsilon \ll 1$, migration induces a fast relaxation on the difference between the mean quantitative traits between the two demes given a major-effect allele: $\bar{z}_{\varepsilon,j}^A - \bar{z}_{\varepsilon,i}^A$ and $\bar{z}_{\varepsilon,j}^a - \bar{z}_{\varepsilon,i}^a$. However, in this study, there is an additional term in the dynamics of the quantitative mean

trait $\overline{z_{\varepsilon,i}^A}$ (resp. $\overline{z_{\varepsilon,i}^a}$): $\left(\frac{\overline{z_{\varepsilon,i}^a} - \overline{z_{\varepsilon,i}^A}}{2}\right) \frac{N_{\varepsilon,i}^a}{N_{\varepsilon,i}}$, which describes how the difference between the mean quantitative trait for alleles A and a within a deme relaxes over time. That is consistent with the result provided by [Proposition 2.1](#).

3 Separation of time scales: slow-fast analysis

The objective of this section is to show that (17) converges when $\varepsilon \rightarrow 0$ toward a simplified problem. Let us make the separation of time scales explicit by introducing the following change of variables, which is motivated by the formal analysis of Section 2.1, [Proposition 2.1](#) and Remark 2:

$$\delta_\varepsilon^a = \frac{\overline{z_{\varepsilon,2}^a} - \overline{z_{\varepsilon,1}^a}}{2\varepsilon^2}, \quad \delta_\varepsilon^A = \frac{\overline{z_{\varepsilon,2}^A} - \overline{z_{\varepsilon,1}^A}}{2\varepsilon^2}, \quad \delta_\varepsilon = \frac{\overline{z_{\varepsilon,1}^A} + \overline{z_{\varepsilon,2}^A} - \overline{z_{\varepsilon,1}^a} - \overline{z_{\varepsilon,2}^a}}{4\varepsilon^2}, \quad Z_\varepsilon = \frac{\overline{z_{\varepsilon,1}^A} + \overline{z_{\varepsilon,2}^A} + \overline{z_{\varepsilon,1}^a} + \overline{z_{\varepsilon,2}^a}}{4}. \quad (18)$$

Z_ε can be interpreted as the mean infinitesimal part of the meta population, δ_ε the spatial average of the local difference between the two allelic mean infinitesimal parts, δ_ε^A and δ_ε^a the spatial discrepancies in the mean infinitesimal parts per allele (see an illustration of those new variables in Fig. 2).

Under this change of variable, the system (17) is equivalent to the following:

$$\left\{ \begin{array}{l} \varepsilon^2 \frac{dN_{\varepsilon,i}^a}{dt} = \lambda^{i-1} N_{\varepsilon,i}^a - [N_{\varepsilon,i}^A + N_{\varepsilon,i}^a] N_{\varepsilon,i}^a - g_i [Z_\varepsilon + \eta^a - (-1)^i]^2 N_{\varepsilon,i}^a \\ \quad + \alpha^{(-1)^j} m_j N_{\varepsilon,j}^a - m_i N_{\varepsilon,i}^a + \mathcal{O}(\varepsilon^2), \\ \varepsilon^2 \frac{dN_{\varepsilon,i}^A}{dt} = \lambda^{i-1} N_{\varepsilon,i}^A - [N_{\varepsilon,i}^A + N_{\varepsilon,i}^a] N_{\varepsilon,i}^A - g_i [Z_\varepsilon + \eta^A - (-1)^i]^2 N_{\varepsilon,i}^A \\ \quad + \alpha^{(-1)^j} m_j N_{\varepsilon,j}^A - m_i N_{\varepsilon,i}^A + \mathcal{O}(\varepsilon^2), \\ \varepsilon^2 \frac{d\delta_\varepsilon^a}{dt} = g_1 + g_2 + (g_1 - g_2) (Z_\varepsilon + \eta^a) + \frac{\delta_\varepsilon}{2} \left[\frac{N_{\varepsilon,2}^A}{N_{\varepsilon,2}^a + N_{\varepsilon,2}^A} - \frac{N_{\varepsilon,1}^A}{N_{\varepsilon,1}^a + N_{\varepsilon,1}^A} \right] \\ \quad - \delta_\varepsilon^a \left[\frac{m_2 \alpha N_{\varepsilon,2}^a}{N_{\varepsilon,1}^a} + \frac{m_1 N_{\varepsilon,1}^a}{\alpha N_{\varepsilon,2}^a} \right] + \frac{\delta_\varepsilon^A - \delta_\varepsilon^a}{4} \left[\frac{N_{\varepsilon,2}^A}{N_{\varepsilon,2}^a + N_{\varepsilon,2}^A} + \frac{N_{\varepsilon,1}^A}{N_{\varepsilon,1}^a + N_{\varepsilon,1}^A} \right] + \mathcal{O}(\varepsilon^2), \\ \varepsilon^2 \frac{d\delta_\varepsilon^A}{dt} = g_1 + g_2 + (g_1 - g_2) (Z_\varepsilon + \eta^A) + \frac{\delta_\varepsilon}{2} \left[\frac{N_{\varepsilon,1}^A}{N_{\varepsilon,1}^a + N_{\varepsilon,1}^A} - \frac{N_{\varepsilon,2}^A}{N_{\varepsilon,2}^a + N_{\varepsilon,2}^A} \right] \\ \quad - \delta_\varepsilon^A \left[\frac{m_2 \alpha N_{\varepsilon,2}^A}{N_{\varepsilon,1}^a} + \frac{m_1 N_{\varepsilon,1}^A}{\alpha N_{\varepsilon,2}^A} \right] + \frac{\delta_\varepsilon^a - \delta_\varepsilon^A}{4} \left[\frac{N_{\varepsilon,2}^A}{N_{\varepsilon,2}^a + N_{\varepsilon,2}^A} + \frac{N_{\varepsilon,1}^A}{N_{\varepsilon,1}^a + N_{\varepsilon,1}^A} \right] + \mathcal{O}(\varepsilon^2), \\ \varepsilon^2 \frac{d\delta_\varepsilon}{dt} = -\frac{\delta_\varepsilon}{2} - (g_1 + g_2) \frac{\eta^A - \eta^a}{2} + \left(\frac{\delta_\varepsilon^A}{2} \left[\frac{\alpha m_2 N_{\varepsilon,2}^A}{N_{\varepsilon,1}^a} - \frac{m_1 N_{\varepsilon,1}^A}{\alpha N_{\varepsilon,2}^A} \right] - \frac{\delta_\varepsilon^a}{2} \left[\frac{\alpha m_2 N_{\varepsilon,2}^a}{N_{\varepsilon,1}^a} - \frac{m_1 N_{\varepsilon,1}^a}{\alpha N_{\varepsilon,2}^a} \right] \right) \\ \quad + \mathcal{O}(\varepsilon^2), \\ \frac{dZ_\varepsilon}{dt} = (g_2 - g_1) - (g_1 + g_2) \left(Z_\varepsilon + \frac{\eta^A + \eta^a}{2} \right) + \frac{\delta_\varepsilon}{2} \left[\frac{N_{1,\varepsilon}^A}{N_{1,\varepsilon}^a + N_{1,\varepsilon}^A} + \frac{N_{2,\varepsilon}^A}{N_{2,\varepsilon}^a + N_{2,\varepsilon}^A} - 1 \right] \\ \quad + \left(\frac{\delta_\varepsilon^a}{2} \left[\frac{\alpha m_2 N_{\varepsilon,2}^a}{N_{\varepsilon,1}^a} - \frac{m_1 N_{\varepsilon,1}^a}{\alpha N_{\varepsilon,2}^a} \right] + \frac{\delta_\varepsilon^A}{2} \left[\frac{\alpha m_2 N_{\varepsilon,2}^A}{N_{\varepsilon,1}^a} - \frac{m_1 N_{\varepsilon,1}^A}{\alpha N_{\varepsilon,2}^A} \right] \right) \\ \quad + \frac{\delta_\varepsilon^A - \delta_\varepsilon^a}{4} \left[\frac{N_{2,\varepsilon}^A}{N_{2,\varepsilon}^a + N_{2,\varepsilon}^A} - \frac{N_{1,\varepsilon}^A}{N_{1,\varepsilon}^a + N_{1,\varepsilon}^A} \right] + \mathcal{O}(\varepsilon^2). \end{array} \right. \quad (19)$$

The system (19) is in a suitable form for a slow-fast analysis when $\varepsilon \rightarrow 0$. Indeed, denoting $\Omega = (\mathbb{R}_+^*)^4 \times \mathbb{R}^3$, there exists $G \in C^\infty(\Omega \times \mathbb{R})$ and $F \in C^\infty(\Omega)$ such that (19) is equivalent to the more compactly written slow-fast system:

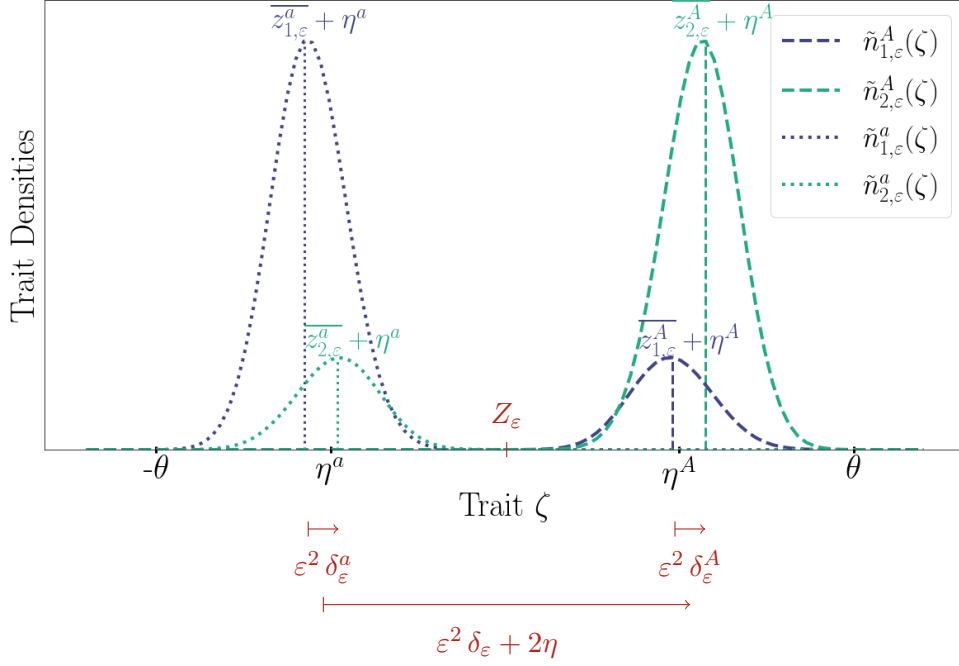


Figure 2: **Illustration of the slow-fast variables Z_ϵ , δ_ϵ , δ_ϵ^A and δ_ϵ^a (in red)**, introduced in (18). This figure displays a situation where both major alleles are segregating in both demes in a symmetrical fashion. The main graph represents the two local trait densities for each of the two alleles: $\tilde{n}_{1,\epsilon}^A$, $\tilde{n}_{2,\epsilon}^A$, $\tilde{n}_{1,\epsilon}^a$, $\tilde{n}_{2,\epsilon}^a$ (the same color is for the same deme, and the same linestyle is for the same major allele), as a function of the trait $\zeta = z + \eta^A$ (resp. $z + \eta^a$, where z is the infinitesimal contribution and η^A (resp η^a) is the effect of the major allele). In red, we indicate a visualization of the new variables introduced in (18). Z_ϵ is the mean infinitesimal part of the metapopulation, δ_ϵ the spatial average of the local difference between the two allelic mean infinitesimal parts, δ_ϵ^A and δ_ϵ^a the spatial discrepancies in the mean infinitesimal parts per allele. Note the difference in notation between the trait densities $\tilde{n}_{i,\epsilon}^A$ and the infinitesimal contribution densities $n_{i,\epsilon}^A$ (which are the ones used in the analysis), which are linked by $n_{i,\epsilon}^A(z) = \tilde{n}_{i,\epsilon}^A(z + \eta^A)$ (respectively $z + \eta^a$ for $\tilde{n}_{i,\epsilon}^a$).

$$\begin{cases} \varepsilon^2 \frac{d\bar{Y}_\varepsilon}{dt} = G(\bar{Y}_\varepsilon, Z_\varepsilon) + \varepsilon^2 \nu_\varepsilon^G(t), \\ \frac{dZ_\varepsilon}{dt} = -(g_1 + g_2) Z_\varepsilon + F(\bar{Y}_\varepsilon) + \varepsilon^2 \nu_\varepsilon^F(t), \end{cases} \quad (P_\varepsilon)$$

where $\bar{Y}_\varepsilon = (N_{1,\varepsilon}^a, N_{1,\varepsilon}^A, N_{2,\varepsilon}^a, N_{2,\varepsilon}^A, \delta_\varepsilon^a, \delta_\varepsilon^A, \delta_\varepsilon)$ denotes the elements of Ω , and ν_ε^F and ν_ε^G are residues, uniformly bounded with respect to ε when ε vanishes. The first equation of (P_ε) happens on a fast ecological timescale and drives the dynamics of the ecological part of the system, whereas the second equation acts on a slow evolutionary time scale, driving the dynamics of Z_ε .

This section is dedicated to show that the solutions of (P_ε) converge when ε goes to 0, toward the solutions of the limit system:

$$\begin{cases} G(\bar{Y}, Z) = 0, \\ \frac{dZ}{dt} = -(g_1 + g_2) Z + F(\bar{Y}). \end{cases} \quad (P_0)$$

We can interpret this limit system (P_0) as the dynamics of the slow variable Z that occurs on the slow manifold defined by the algebraic system $G(\bar{Y}, Z) = 0$. Its solutions are the instantaneous ecological equilibria \bar{Y} given the slow variable Z . The convergence is stated by the following:

Theorem 3.1. *For (\bar{Y}, Z) a solution of (P_0) , there exists $T^* > 0$ such that, for $0 < \varepsilon < 1$, any solution $(\bar{Y}_\varepsilon, Z_\varepsilon)$ of (P_ε) on $[0, T^*]$ converges to (\bar{Y}, Z) uniformly on $[0, T^*]$, as ε goes to 0 and $(\bar{Y}_\varepsilon(0), Z_\varepsilon(0))$ goes to $(\bar{Y}(0), Z(0))$.*

The arguments of the proof of Theorem 3.1 are similar to the analogous theorems proved in Levin and Levinson (1954) and Dekens (2020). The proof requires some preliminaries results, particularly of stability, to which we dedicate the rest of this section. The structure of this section is represented in Fig. 3.

In the rest of this section, we first solve the slow manifold algebraic system $G(\bar{Y}, Z) = 0$, showing that there can only exist one instantaneous ecological equilibrium at a given $Z \in]-1, 1[$ (Proposition 3.1 and Proposition 3.2 of Section 3.1.1). Surprisingly, this resolution is easier than the analogous one in Dekens (2020) (see Remark 4). Next, in Section 3.1.2, we show a stability criterion of the slow manifold (Proposition 3.3 and Proposition 3.4), which justifies the separation of time scales approach.

Remark 3 (One-locus haploid model's equilibrium is a fast equilibrium). *One can notice that the one-locus haploid model is equivalent to the first four differential equations of (19) on the allelic sizes of each subpopulation, when $Z_\varepsilon = 0$ (no infinitesimal part) (we can obtain from these equations a system describing the allelic frequencies and local population sizes $(p_1, p_2, N_1, N_2) := \left(\frac{N_1^A}{N_1^A + N_1^a}, \frac{N_2^A}{N_2^A + N_2^a}, N_1^A + N_1^a, N_2^A + N_2^a \right)$, dropping the ε that is a parameter of the infinitesimal part). Applying Proposition 3.1 with $Z = 0$ gives a unique equilibrium satisfying the first four equations, which is the one found with the one-locus haploid model. One can thus interpret the symmetrical polymorphic equilibrium of the one-locus haploid model as a fast equilibrium in the model presented in this article. It is therefore stable (Proposition 3.3) whenever it entails positive population sizes (same condition as in Proposition 3.1).*

3.1 Analysis of the fast equilibria.

The fast equilibria, for $Z \in]-1, 1[$, are defined as the solutions \bar{Y} to the algebraic system $G(\bar{Y}, Z) = 0$, or equivalently seven equations that we group in two subsystems $S_0(Z)$ and

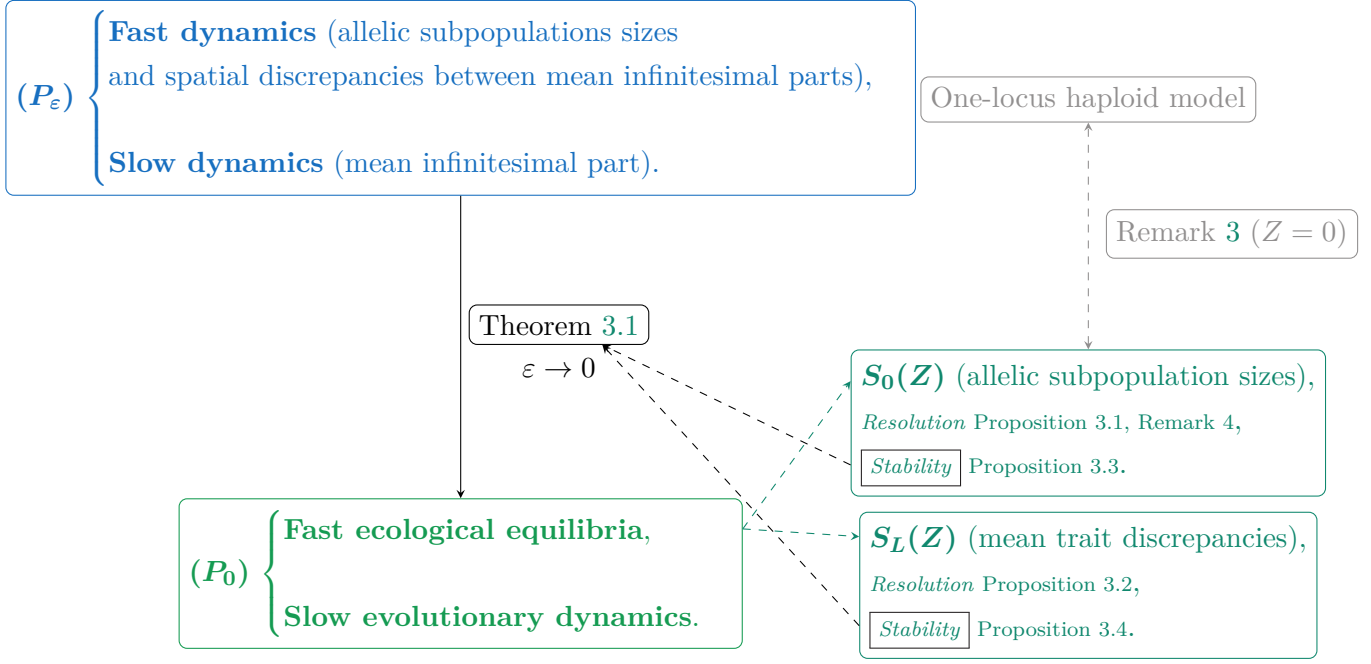


Figure 3: **Layout of the slow-fast analysis in Section 3.** This figure presents the key elements of the separation of time scales leading from P_ε to P_0 . The stability of the fast equilibria (studied in the two subsystems $S_0(Z)$ and $S_L(Z)$) is the crucial argument underlying the convergence result stated in Theorem 3.1. The resolution of $S_0(Z)$ leads to a uniqueness result that is unexpected with regard to the analogous resolution in Dekens (2020) (see Remark 4).

$S_L(Z)$:

$$\begin{cases} \alpha m_2 N_2^a - m_1 N_1^a + N_1^a \left[1 - (N_1^a + N_1^A) - g_1 (Z + \eta^a + 1)^2 \right] & = 0, \\ \alpha m_2 N_2^A - m_1 N_1^A + N_1^A \left[1 - (N_1^a + N_1^A) - g_1 (Z + \eta^A + 1)^2 \right] & = 0, \\ \frac{m_1}{\alpha} N_1^a - m_2 N_2^a + N_2^a \left[\lambda - (N_2^a + N_2^A) - g_2 (Z + \eta^a - 1)^2 \right] & = 0, \\ \frac{m_1}{\alpha} N_1^A - m_2 N_2^A + N_2^A \left[\lambda - (N_2^a + N_2^A) - g_2 (Z + \eta^A - 1)^2 \right] & = 0. \end{cases} \quad (S_0(Z))$$

$$J_{S_L} \begin{pmatrix} \delta \\ \delta^A \\ \delta^a \end{pmatrix} = \begin{pmatrix} (g_1 + g_2) \frac{\eta^A - \eta^a}{2} \\ -(g_1 + g_2) + (g_2 - g_1)(Z + \eta^A) \\ -(g_1 + g_2) + (g_2 - g_1)(Z + \eta^a) \end{pmatrix}, \quad (S_L(Z))$$

where:

$$J_{S_L} := \begin{pmatrix} -\frac{1}{2} & \frac{1}{2} \left[\frac{\alpha m_2 N_2^A}{N_1^A} - \frac{m_1 N_1^A}{\alpha N_2^A} \right] & -\frac{1}{2} \left[\frac{\alpha m_2 N_2^a}{N_1^a} - \frac{m_1 N_1^a}{\alpha N_2^a} \right] \\ \frac{\frac{N_1^a}{N_1^A + N_1^a} - \frac{N_2^a}{N_2^A + N_2^a}}{2} & - \left[\frac{\alpha m_2 N_2^A}{N_1^A} + \frac{m_1 N_1^A}{\alpha N_2^A} \right] - \frac{\frac{N_1^a}{N_1^A + N_1^a} + \frac{N_2^a}{N_2^A + N_2^a}}{4} & \frac{\frac{N_1^a}{N_1^A + N_1^a} + \frac{N_2^a}{N_2^A + N_2^a}}{4} \\ \frac{\frac{N_2^A}{N_2^A + N_2^a} - \frac{N_1^A}{N_1^A + N_1^a}}{2} & \frac{\frac{N_1^A}{N_1^A + N_1^a} + \frac{N_2^A}{N_2^A + N_2^a}}{4} & - \left[\frac{\alpha m_2 N_2^a}{N_1^a} + \frac{m_1 N_1^a}{\alpha N_2^a} \right] - \frac{\frac{N_1^A}{N_1^A + N_1^a} + \frac{N_2^A}{N_2^A + N_2^a}}{4} \end{pmatrix}$$

3.1.1 Resolution.

Following Working assumption 1, we recall that we assume that no major allele has fixed. Here, we show that there is at most one instantaneous ecological equilibrium at each Z -level (for $Z \in]-1 - \frac{\eta^A + \eta^a}{2}, 1 - \frac{\eta^A + \eta^a}{2}[$), thanks to Proposition 3.1 and Proposition 3.2.

Proposition 3.1. Suppose that no major allele has fixed. Then, for $Z \in]-1 - \frac{\eta^A + \eta^a}{2}, 1 - \frac{\eta^A + \eta^a}{2}[$, $S_0(Z)$ has exactly one solution $(N_1^a, N_1^A, N_2^a, N_2^A) \in (\mathbb{R}^*)^4$, given by:

$$N_1^a = \frac{Y^A N_1 - N_2}{Y^A - Y^a}, \quad N_2^a = Y^a \frac{Y^A N_1 - N_2}{Y^A - Y^a}, \quad N_1^A = \frac{N_2 - Y^a N_1}{Y^A - Y^a}, \quad N_2^A = Y^A \frac{N_2 - Y^a N_1}{Y^A - Y^a},$$

where the quantities (Y^A, Y^a, N_1, N_2) are defined by (20):

$$\begin{cases} Y^A = \frac{g_1}{\alpha m_2} \left(\eta^A + \eta^a + 2(Z+1) \right) \frac{\eta^A - \eta^a}{2} \left[\sqrt{1 + \frac{m_1 m_2}{4 g_1 g_2 \left(\frac{\eta^A - \eta^a}{2} \right)^2 \left(1 - \left(\frac{\eta^A + \eta^a}{2} + Z \right)^2 \right)} + 1 \right], \\ Y^a = \frac{g_1}{\alpha m_2} \left(\eta^A + \eta^a + 2(Z+1) \right) \frac{\eta^A - \eta^a}{2} \left[\sqrt{1 + \frac{m_1 m_2}{4 g_1 g_2 \left(\frac{\eta^A - \eta^a}{2} \right)^2 \left(1 - \left(\frac{\eta^A + \eta^a}{2} + Z \right)^2 \right)} - 1 \right], \\ N_1 = 1 - g_1 (Z+1 + \eta^A)^2 - m_1 + \alpha m_2 Y^A, \\ N_2 = \lambda - g_2 (Z-1 + \eta^A)^2 - m_2 + \frac{m_1}{\alpha Y^A}. \end{cases} \quad (20)$$

This solution $(N_1^a, N_1^A, N_2^a, N_2^A)$ defines viable numbers of each allele in each sub-populations if and only if:

$$[Y^A N_1 > N_2] \text{ and } [N_2 > Y^a N_1]. \quad (21)$$

Remark 4 (Degrees of freedom of $S_0(Z)$). *Proposition 3.1* states that there are fewer degrees of freedom in $S_0(Z)$ than in the analogous system of two equations from the analysis done in Dekens (2020), that can be obtained in the case where one allele has fixed (up to a translation). Indeed, Dekens (2020) shows that the analogous system can have up to three algebraic solutions depending on the parameters. The result of *Proposition 3.1* is thus unexpected, since $S_0(Z)$ has twice the number of equations and variables.

Proof. Let us introduce the following change of variables, valid under the assumption that no major allele has fixed:

$$N_1 := N_1^A + N_1^a, \quad N_2 := N_2^A + N_2^a, \quad Y^A := \frac{N_2^A}{N_1^A}, \quad Y^a := \frac{N_2^a}{N_1^a}.$$

Then, under the assumptions made in Working assumption 1, the system $(S_0(Z))$ is equivalent to:

$$\begin{cases} \alpha m_2 Y^a - m_1 + [1 - N_1 - g_1 (Z + \eta^a + 1)^2] = 0, \\ \alpha m_2 Y^A - m_1 + [1 - N_1 - g_1 (Z + \eta^A + 1)^2] = 0, \\ \frac{m_1}{\alpha} \frac{1}{Y^a} - m_2 + [\lambda - N_2 - g_2 (Z + \eta^a - 1)^2] = 0, \\ \frac{m_1}{\alpha} \frac{1}{Y^A} - m_2 + [\lambda - N_2 - g_2 (Z + \eta^A - 1)^2] = 0. \end{cases} \quad (22)$$

This is equivalent to the following system:

$$\begin{cases} \alpha m_2 (Y^a - Y^A) + g_1 \left(\eta^A + \eta^a + 2(Z+1) \right) (\eta^A - \eta^a) = 0, \\ \frac{m_1}{\alpha} \left(\frac{1}{Y^a} - \frac{1}{Y^A} \right) + g_2 \left(\eta^A + \eta^a + 2(Z-1) \right) (\eta^A - \eta^a) = 0, \\ N_1 - \left(1 - g_1 (Z+1 + \eta^A)^2 - m_1 + \alpha m_2 Y^A \right) = 0, \\ N_2 - \left(\lambda - g_2 (Z-1 + \eta^A)^2 - m_2 + \frac{m_1}{\alpha Y^A} \right) = 0. \end{cases}$$

As $Z \neq 1 - \frac{\eta^A + \eta^a}{2}$, the closed subsystem on (Y^A, Y^a) is, in turn, equivalent to:

$$\begin{cases} Y^A - Y^a &= A_1(Z) := \frac{g_1}{\alpha m_2} \left(\eta^A + \eta^a + 2(Z+1) \right) (\eta^A - \eta^a), \\ -Y^A Y^a &= A_0(Z) := \frac{g_1 m_1}{\alpha^2 g_2 m_2} \frac{\eta^A + \eta^a + 2(Z+1)}{\eta^A + \eta^a + 2(Z-1)}. \end{cases}$$

Y^A and $-Y^a$ are the roots of the polynomial:

$$P(X) = X^2 - A_1(Z) X + A_0(Z).$$

P has two real roots of opposite signs if and only if:

$$[A_0(Z) < 0],$$

which is equivalent to:

$$-1 - \frac{\eta^A + \eta^a}{2} < Z < 1 - \frac{\eta^A + \eta^a}{2}.$$

Under the last condition on Z , $A_1(Z)$ is positive, $A_0(Z)$ is negative and we get:

$$\begin{cases} Y^A = \frac{A_1(Z)}{2} \left[\sqrt{1 - \frac{A_0(Z)}{\left(\frac{A_1(Z)}{2}\right)^2}} + 1 \right], \\ Y^a = \frac{A_1(Z)}{2} \left[\sqrt{1 - \frac{A_0(Z)}{\left(\frac{A_1(Z)}{2}\right)^2}} - 1 \right], \end{cases} \quad (23)$$

which is equivalent to (20).

Inverting the initial change of variables leads to:

$$N_1^a = \frac{Y^A N_1 - N_2}{Y^A - Y^a}, \quad N_2^a = Y^a \frac{Y^A N_1 - N_2}{Y^A - Y^a}, \quad N_1^A = \frac{N_2 - Y^a N_1}{Y^A - Y^a}, \quad N_2^A = Y^A \frac{N_2 - Y^a N_1}{Y^A - Y^a},$$

hence (20). It defines a viable solution with positive entries if and only if $Y^A N_1 > N_2$ and $N_2 > Y^a N_1$. \square

Proposition 3.2. *For all allelic sizes of subpopulations $(N_1^a, N_1^A, N_2^a, N_2^A) \in (\mathbb{R}_+^*)^4$, there exists a unique solution $(\delta, \delta^A, \delta^a)$ to the system $S_L(Z)$.*

Proof. Using the notation $N_1 := N_1^A + N_1^a$ and $N_2 := N_2^A + N_2^a$, we compute thanks to a symbolic computation tool (Mathematica©):

$$\begin{aligned} \det(J_{S_L}) &= -\frac{1}{4} \left[\frac{m_1}{\alpha} \frac{N_1}{N_2} + \alpha m_2 \frac{N_2}{N_1} + 2 \frac{m_1^2}{\alpha^2} \frac{N_1^a N_1^A}{N_2^a N_2^A} + 2 \alpha^2 m_2^2 \frac{N_2^a N_2^A}{N_1^a N_1^A} \right. \\ &\quad \left. + 2 m_1 m_2 \left(\frac{N_1^{A^2} N_2^a}{N_1^a N_1 N_2} + \frac{N_1^{a^2} N_2^A}{N_1^A N_1 N_2} + \frac{N_2^{A^2} N_1^a}{N_2^a N_1 N_2} + \frac{N_2^{a^2} N_1^A}{N_2^A N_1 N_2} + 2 \frac{N_2^A N_1^a}{N_1 N_2} + 2 \frac{N_1^a N_2^A}{N_1 N_2} \right) \right] \\ &< 0. \end{aligned}$$

\square

3.1.2 Stability.

Convergence toward a limit system locally in time in a slow-fast analysis relies essentially on a stability criterion of the fast equilibria which constitute the slow manifold (Levin and Levinson 1954; Dekens 2020). In this subsection, we show that all fast equilibria found in Proposition 3.1 and Proposition 3.2 for a level $Z \in]-1 - \frac{\eta^A + \eta^a}{2}, 1 - \frac{\eta^A + \eta^a}{2}[$, are stable. Due to the particular shape of the slow manifold, it is sufficient to study separately the Jacobian matrix associated to $S_0(Z)$ denoted J_{S_0} (Proposition 3.3) and the Jacobian matrix associated to the linear system $S_L(Z)$, which is exactly J_{S_L} (Proposition 3.4).

Proposition 3.3. *Let $Z \in]-1 - \frac{\eta^A + \eta^a}{2}, 1 - \frac{\eta^A + \eta^a}{2}[$ such that $(S_0(Z))$ has a unique solution $(N_1^a, N_1^A, N_2^a, N_2^A) \in (\mathbb{R}_+^*)^4$. Let us define the following matrix:*

$$J_{S_0} = \begin{pmatrix} -\frac{\alpha m_2 N_2^a}{N_1^a} - N_1^a & \alpha m_2 & -N_1^a & 0 \\ \frac{m_1}{\alpha} & -\frac{m_1 N_1^a}{\alpha N_2^a} - N_2^a & 0 & -N_2^a \\ -N_1^A & 0 & -\frac{\alpha m_2 N_2^A}{N_1^A} - N_1^A & \alpha m_2 \\ 0 & -N_2^A & \frac{m_1}{\alpha} & -\frac{m_1 N_1^A}{\alpha N_2^A} - N_2^A \end{pmatrix}. \quad (24)$$

Then:

1. J_{S_0} is the Jacobian of $S_0(Z)$ at $(N_1^a, N_1^A, N_2^a, N_2^A)$.
2. All the eigenvalues of J_{S_0} are located in the left open half plane.

Proof. 1. Let $(N_1^a, N_1^A, N_2^a, N_2^A)$ be solution of $S_0(Z)$. One can verify that:

$$\begin{aligned} & \frac{\partial \left[\alpha m_2 N_2^a - m_1 N_1^a + N_1^a \left[1 - (N_1^a + N_1^A) - g_1 (Z + \eta^a + 1)^2 \right] \right]}{\partial N_1^a} \\ &= \left[1 - (N_1^a + N_1^A) - g_1 (Z + \eta^a + 1)^2 - m_1 \right] - N_1^a = -\frac{\alpha m_2 N_2^a}{N_1^a} - N_1^a, \end{aligned}$$

for $(N_1^a, N_1^A, N_2^a, N_2^A)$ solves $S_0(Z)$. The same holds for the other diagonal entries.

2. Let:

$$\chi_{J_{S_0}}(X) = X^4 - \text{tr}(J_{S_0}) X^3 + b X^2 + c X + \det J_{S_0},$$

be the characteristic polynomial of J_{S_0} . Let us verify the Routh-Hurwitz criterion: all the eigenvalues of J_{S_0} are located in the left open half plane if and only if:

- (i) $\det J_{S_0} > 0$,
- (ii) $-\text{tr}(J_{S_0}) > 0$,
- (iii) $-\text{tr}(J_{S_0}) b - c > 0$,
- (iv) $(-\text{tr}(J_{S_0}) b - c) c - \text{tr}(J_{S_0})^2 \det J_{S_0} > 0$.

We have:

$$\det J_{S_0} = m_1 m_2 \left(N_1^a N_2^a - N_1^A N_2^A \right)^2 \left(\frac{1}{N_1^a N_2^A} + \frac{1}{N_1^A N_2^a} \right) > 0.$$

and:

$$-\operatorname{tr}(J_{S_0}) = N_1 + N_2 + \sqrt{m_1 m_2} \left(\frac{\alpha \sqrt{m_2} N_2^a}{\sqrt{m_1} N_1^a} + \frac{\sqrt{m_1} N_1^a}{\alpha \sqrt{m_2} N_2^a} + \frac{\alpha \sqrt{m_2} N_2^A}{\sqrt{m_1} N_1^A} + \frac{\alpha \sqrt{m_2} N_2^A}{\sqrt{m_1} N_1^A} \right) > 0.$$

With the help of a symbolic computation tool (Mathematica©), we verify that the left hand side of the two last conditions are sums of positive terms, but are too long to be displayed here. \square

The Jacobian matrix of the linear system $\mathcal{S}_L(Z)$ is exactly J_{S_L} and we also show that J_{S_L} satisfies the Routh-Hurwitz criterion:

Proposition 3.4. *J_{S_L} has all its eigenvalues located in the left open half plane.*

Proof. Let the following be the characteristic polynomial of J_{S_L} :

$$\chi_{J_{S_L}}(X) = X^3 - \operatorname{tr}(J_{S_L})X^2 - \frac{1}{2} \left(\operatorname{tr}(J_{S_L}^2) - \operatorname{tr}(J_{S_L})^2 \right) X - \det(J_{S_L}).$$

We show that J_{S_L} satisfies the Routh-Hurwitz criterion:

- (i) $-\det(J_{S_L}) > 0$,
- (ii) $-\operatorname{tr}(J_{S_L}) > 0$,
- (iii) $\frac{1}{2} \left(\operatorname{tr}(J_{S_L}^2) - \operatorname{tr}(J_{S_L})^2 \right) \operatorname{tr}(J_{S_L}) + \det(J_{S_L}) > 0$.

We have $-\det(J_{S_L}) > 0$ from the proof of [Proposition 3.2](#) and:

$$-\operatorname{tr}(J_{S_L}) = 1 + \sqrt{m_1 m_2} \left(\frac{\alpha \sqrt{m_2} N_2^a}{\sqrt{m_1} N_1^a} + \frac{\sqrt{m_1} N_1^a}{\alpha \sqrt{m_2} N_2^a} + \frac{\alpha \sqrt{m_2} N_2^A}{\sqrt{m_1} N_1^A} + \frac{\alpha \sqrt{m_2} N_2^A}{\sqrt{m_1} N_1^A} \right) > 1 + 4\sqrt{m_1 m_2}.$$

We verify that the l.h.s. of the last condition is a sum of positive terms. \square

4 Stability of polymorphism in the limit system

This section follows naturally the result given by [Theorem 3.1](#) by being dedicated to the study of the stability of polymorphism at the major effect locus. To be able to derive analytical conditions, we assume henceforth a symmetrical setting (in migration rates, selection strengths, carrying capacities, reproduction rates and major allelic effects):

$$m := m_1 = m_2, \quad g := g_1 = g_2, \quad \alpha = 1, \quad \lambda = 1, \quad \eta := \eta^A = -\eta^a > 0.$$

Under these symmetrical conditions, there can exist a symmetrical polymorphic equilibrium, that we henceforth denote (Z_0, \bar{Y}_0) , where $Z_0 = 0$. Recall that the first four coordinates of \bar{Y}_0 , which are the allelic sizes of subpopulations, are shared with the one-locus haploid model (see [Remark 3](#)). The results of this section show that the unconditional stability of the polymorphism in the one-locus haploid model can be disturbed by the presence of an infinitesimal background, for a substantial range of parameters. The interpretation of [Remark 3](#) offers the idea that the infinitesimal background slowly disrupts the fast established symmetrical polymorphism at the major locus.

We first show that a symmetrical polymorphic equilibrium can exist under a range of parameters specified in [Proposition 4.1](#), as a stationary state of the limit system, hence a solution of (25):

$$\begin{cases} N_i^a - \left[N_i^A + N_i^a \right] N_i^a - g \left[Z - \eta - (-1)^i \right]^2 N_i^a + m(N_j^a - N_i^a) = 0, \\ N_i^A - \left[N_i^A + N_i^a \right] N_i^A - g \left[Z + \eta - (-1)^i \right]^2 N_i^A + m(N_j^A - N_i^A) = 0, \\ 2g - m \delta^a \left[\frac{N_2^a}{N_1^a} + \frac{N_1^a}{N_2^a} \right] + \frac{\delta^A - \delta^a}{4} \left[\frac{N_2^A}{N_2^a + N_2^A} + \frac{N_1^A}{N_1^a + N_1^A} \right] + \frac{\delta}{2} \left[\frac{N_2^A}{N_2^a + N_2^A} - \frac{N_1^A}{N_1^a + N_1^A} \right] = 0, \\ 2g - m \delta^A \left[\frac{N_2^A}{N_1^A} + \frac{N_1^A}{N_2^A} \right] + \frac{\delta^a - \delta^A}{4} \left[\frac{N_2^a}{N_2^a + N_2^A} + \frac{N_1^a}{N_1^a + N_1^A} \right] + \frac{\delta}{2} \left[\frac{N_1^A}{N_2^a + N_2^A} - \frac{N_2^a}{N_1^a + N_1^A} \right] = 0, \\ -\frac{\delta}{2} - 2g\eta + m \left(\frac{\delta^A}{2} \left[\frac{N_2^A}{N_1^A} - \frac{N_1^A}{N_2^A} \right] - \frac{\delta^a}{2} \left[\frac{N_2^a}{N_1^a} - \frac{N_1^a}{N_2^a} \right] \right) = 0, \\ -2gZ + m \left(\frac{\delta^a}{2} \left[\frac{N_2^a}{N_1^a} - \frac{N_1^a}{N_2^a} \right] + \frac{\delta^A}{2} \left[\frac{N_2^A}{N_1^A} - \frac{N_1^A}{N_2^A} \right] \right) + \frac{\delta^A - \delta^a}{4} \left[\frac{N_2^A}{N_2^a + N_2^A} - \frac{N_1^A}{N_1^a + N_1^A} \right] \\ + \frac{\delta}{2} \left[\frac{N_1^A}{N_1^a + N_1^A} + \frac{N_2^A}{N_2^a + N_2^A} - 1 \right] = 0. \end{cases} \quad (25)$$

Next, we give the condition under which it is stable.

Resolution.

Proposition 4.1. *There exists a unique polymorphic equilibrium corresponding to the infinitesimal average $Z = 0$ under the condition:*

$$\left[g(\eta^2 + 1) < 1 \right] \vee \left[m < \frac{2g^2\eta^2}{g(\eta^2 + 1) - 1} - g(\eta^2 + 1) + 1 \right]. \quad (26)$$

The allelic local population sizes corresponding to this equilibrium satisfy the property:

$$N_{1,0}^a = N_{2,0}^A, \quad N_{2,0}^a = N_{1,0}^A,$$

and for both alleles, the spatial discrepancies between the mean infinitesimal parts of the two demes per allele are the same:

$$\delta_0^A = \delta_0^a.$$

Therefore, this polymorphic equilibrium at $Z = 0$ is called symmetrical.

Proof. Let us define the quantities:

$$\begin{cases} Y_0^A = \frac{2g\eta}{m} \left[\sqrt{1 + \frac{m^2}{4g^2\eta^2}} + 1 \right], \\ Y_0^a = \frac{2g\eta}{m} \left[\sqrt{1 + \frac{m^2}{4g^2\eta^2}} - 1 \right], \\ N_{1,0} = 1 - g\eta^2 - g - m + 2g\eta \sqrt{1 + \frac{m^2}{4g^2\eta^2}}, \\ N_{2,0} = N_{1,0}. \end{cases} \quad (27)$$

[Proposition 3.1](#) states that the latter defines a solution to $S_0(Z)$ given that $Z = 0$:

$$(N_{1,0}^a, N_{2,0}^a, N_{1,0}^A, N_{2,0}^A) = \left(N_{1,0} \frac{Y_0^A - 1}{Y_0^A - Y_0^a}, N_{1,0} \frac{1 - Y_0^a}{Y_0^A - Y_0^a}, N_{1,0} \frac{1 - Y_0^a}{Y_0^A - Y_0^a}, N_{1,0} \frac{Y_0^A - 1}{Y_0^A - Y_0^a} \right).$$

Since $Y_0^A > 1$ and $Y_0^A Y_0^a = 1$, this solution is viable under the condition: $N_{1,0} > 0$, hence requiring :

$$1 + \sqrt{4g^2\eta^2 + m^2} > g\eta^2 + g + m,$$

which in turn is equivalent to (26).

Proposition 3.2 next states that $S_L(Z)$ has a unique solution $(\delta_0, \delta_0^A, \delta_0^a)$ for such allelic population sizes $(N_{1,0}^a, N_{2,0}^a, N_{1,0}^A, N_{2,0}^A)$. One can compute that:

$$\delta_0^A = \delta_0^a = \frac{g(1 + \eta + Y_0^A(1 - \eta))}{m(1 + Y_0^A)}, \quad \delta_0 = -\frac{2g(1 + \eta - Y_0^{A^2}(1 - \eta))}{Y_0^A}.$$

Finally, one can verify that $(N_{1,0}^a, N_{2,0}^a, N_{1,0}^A, N_{2,0}^A, \delta_0, \delta_0^A, \delta_0^a)$ along with setting $Z = 0$ is a solution of the last equation of (25). \square

Stability. Let us recall the limit system (P_0) :

$$\begin{cases} G(\bar{Y}, Z) = 0, \\ \frac{dZ}{dt} = -2gZ + F(\bar{Y}). \end{cases} \quad (28)$$

Stability of the symmetrical polymorphic equilibrium (denoted $(0, \bar{Y}_0)$) described in [Proposition 4.1](#) is studied in the same manner as in [Dekens \(2020\)](#). Thanks to the implicit function theorem used in the vicinity of the symmetrical polymorphic equilibrium, this equilibrium is asymptotically locally stable if and only if:

$$0 < 2g + \partial_{\bar{Y}} F \cdot \left([\partial_{\bar{Y}} G]^{-1} \partial_Z G \right) \Big|_{Z=0, \bar{Y}=\bar{Y}_0}.$$

Due to the large number of dimensions involved, the explicit formula is too long to be given here.

However, we provide numerical analysis results of the stability, displayed in [Fig. 4](#). We show the stability region in yellow for four values of the effect of the major locus $\eta \in \{0.5, 0.7, 1, 1.3\}$, with selection strength (g , x -axis) and migration rate (m , y -axis) varying in $[0, 3]$. For each value of η , we can observe that the symmetrical polymorphic equilibrium is not stable under weak selection. Moreover, at weak to strong migration, stability exhibits non-monotonic behaviour when selection is increasing. Stability is gained at an intermediate level of selection that depends on the migration rate and lost at a higher level of selection. It is worth recalling that the one-locus haploid model predicts that the equilibrium is stable, regardless of selection and migration in this symmetrical case as long as the population does not go extinct (under the dashed curve) (see [Remark 3](#)). Therefore, the instability observed in this model results from the small-effect loci.

Pushing further the numerical analysis of polymorphic equilibria. Here, we show a numerical analysis of all the equilibria of the limit system (P_0) in [Fig. 5](#).

Suppose that the parameters allow for the symmetrical polymorphic equilibrium to exist, i.e. satisfy (26). From the explicit resolution of the fast ecological equilibrium given an evolutionary state $Z \in]-1, 1[$ ([Proposition 3.1](#) and [Proposition 3.2](#)), we deduce, thanks to the implicit function theorem, that there exists an open interval I centered in 0 and a smooth function $\bar{Y} : I \rightarrow \mathbb{R}_+^4 \times \mathbb{R}^3$, which links an evolutionary state Z to its corresponding ecological

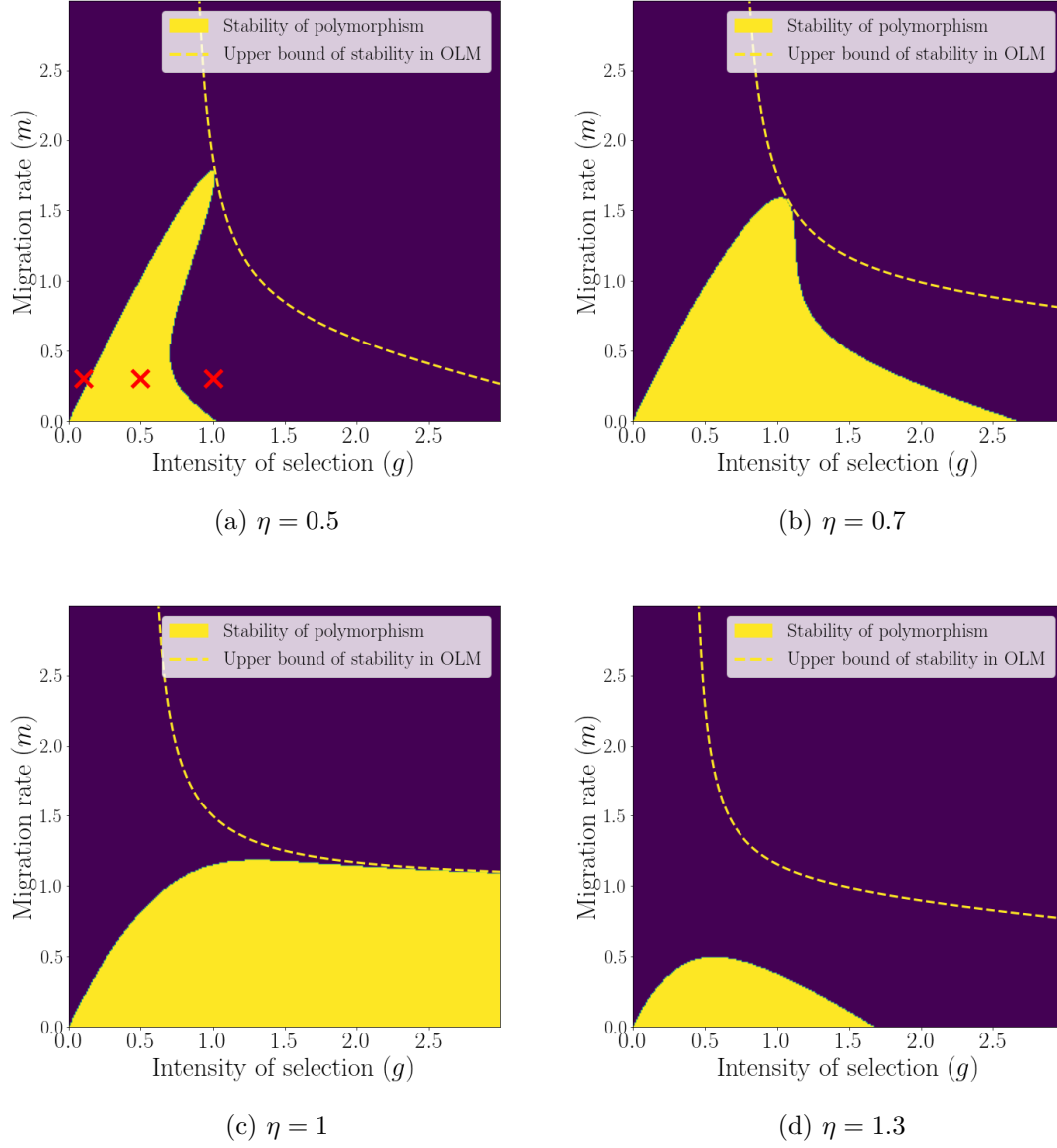


Figure 4: **Stability region of the symmetrical polymorphic equilibrium (in yellow), for four major locus effects $\eta \in \{0.5, 0.7, 1, 1.3\}$** (recalling that $\theta = 1$), when m (y -axis) and g (x -axis) vary in $[0, 3]$. This figure highlights the gain and loss of polymorphism with regard to increasing selection, which is not predicted by the one-locus model (abbreviated as OLM in the legend). The stable region (in yellow) becomes larger as η grows closer to 1, as the major allele effect can then fully explain the divergence between the two demes, then shrinks again. The red crosses in Fig. 4a indicate the parameters used for the individual-based simulations (see Section 5 and Fig. 6).

equilibrium $\bar{Y}(Z)$ (solving $G(\bar{Y}(Z), Z) = 0$). The system (P_0) can thus be represented by the following autonomous differential equation:

$$\frac{dZ}{dt} = \mathcal{F}(Z) := -2gZ + F(\bar{Y}(Z)). \quad (29)$$

Hence, a couple $(Z, \bar{Y}(Z))$ is a polymorphic equilibrium if $\mathcal{F}(Z) = 0$, and this equilibrium is locally stable if $\mathcal{F}'(Z) < 0$.

Even if the complexity of the limit system is still too great to be analytically solved (due to the implicit nature of the function \bar{Y}), we show in Fig. 5 phase lines corresponding to the autonomous limit equation (29), when the migration rate and the effect size of the major locus are held constant ($m = 0.1, \eta = \frac{1}{2}$) and the selection strength varies (the lighter the color, the stronger the selection). Solid lines indicate that the system is polymorphic, whereas dotted lines indicate that one major allele has fixed. Every intersection of the null horizontal line and a solid colored line with a negative slope indicates a locally stable polymorphic equilibrium (conversely, a positive slope indicates an unstable equilibrium).

This figure is consistent with the analysis of Section 4 and Fig. 4a: at $Z = 0$, all the curves return to 0 ($F(Z)$), confirming that a polymorphic equilibrium exists when the mean contribution of the small-effect loci is 0. Their local slope indicates the stability of this equilibrium (stable if negative, unstable if positive). Furthermore, Fig. 5 gives insights on the existence of asymmetrical polymorphic equilibria. Particularly, it seems that such equilibria exist for a narrow window of intermediate selection strength: the green curve corresponding to $g = 0.86$ displays two mirrored stable asymmetrical polymorphic equilibria at $Z \approx \pm 0.5$ (indicated by the red arrows), which is hard to predict analytically due to the high orders of polynomials involved. Moreover, such equilibria are presumably quite subtle to catch in an individual-based simulations, because the window of selection and the basin of attraction are both narrow. However, this illustrates the new and unsuspected insights that can be obtained from this hybrid model.

5 Individual-based simulations

In this section, we explore some of the insights given by our analysis on the stability of the symmetrical polymorphic equilibrium, using individual-based simulations conducted with the software SLiM (Haller and Messer 2019). We focus on the gain and loss of polymorphism with regard to increasing selection, when $\eta \neq 1$. For each set of parameters, we ran 20 replicate simulations. The results on the major locus are displayed in Fig. 6, both with a quantitative background (left panel) and without (right panel). The simulations confirm that variation is maintained only for intermediate levels of selection (as measured by $p(1-p)$, where p is the local frequency of allele A). The framework of the simulations is detailed as follows.

Populations and habitats. The species is split in two subpopulations living in two different habitats, with local carrying capacity $K = 10^4$. In each habitat, individuals experience selection toward a local trait optimum $\theta_i = (-1)^i$ (for habitat i). Initially, the two subpopulations are at $\frac{4}{5}$ of the local carrying capacity. The genetic information of the individuals of the initial population is set as follows. In each subpopulation, all the individuals have, at the major locus, the allele whose effect is the closest to the optimum of the habitat they are in (η in habitat 2 and $-\eta$ in habitat 1). The infinitesimal background is then set randomly and uniformly.

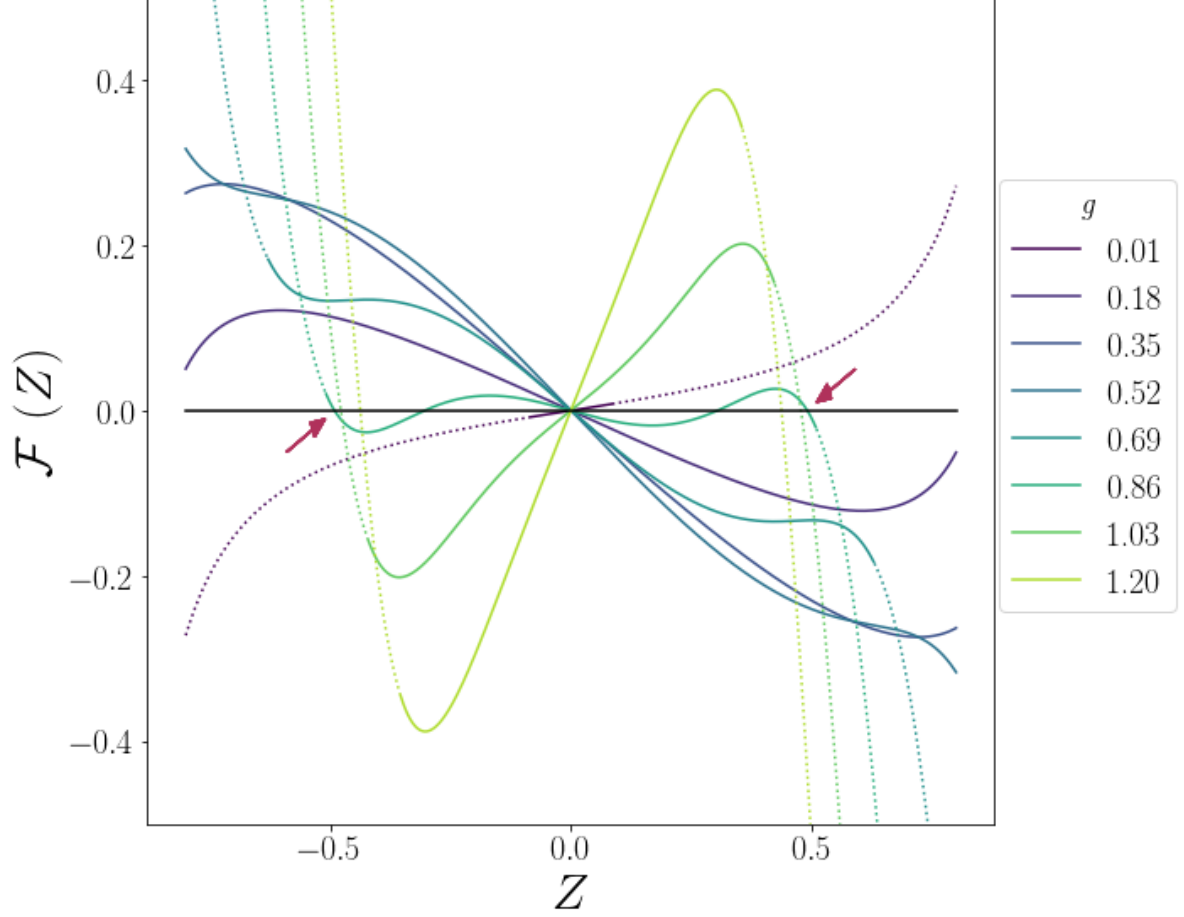


Figure 5: **Phases lines of the autonomous limit equation (29), when the migration rate and the strong effect are held constant ($m = 0.1, \eta = \frac{1}{2}$) and the selection strength varies** (the lighter the color, the stronger the selection). Solid curves indicate that the system is polymorphic, whereas dashed curves indicate that one major allele has fixed. Every intersection of the horizontal black line and a solid colored curve with a negative (resp. positive) slope indicates a locally stable (resp. unstable) polymorphic equilibrium. The darker curve with weak selection $g = 0.01$ has a positive slope at $Z = 0$ (unstable), the following curves have a negative slope at $Z = 0$ (stable for selection between $g = 0.18$ and $g = 0.86$), and finally the lightest curves have a positive slope at $Z = 0$ (unstable for $g \geq 1.03$), which is consistent with Fig. 4a. Note that there exists additionally two mirrored asymmetrical polymorphic equilibria for $g = 0.86$, for $Z \approx \pm 0.5$ (indicated by the red arrows), which were unsuspected prior to this numerical analysis.

Genetic architecture. We consider $L = 500$ unlinked loci constituting the infinitesimal background. At each of these loci, two alleles segregate, having an additive effect on the trait of the individual of value $\frac{\sigma}{\sqrt{L}}$ or $-\frac{\sigma}{\sqrt{L}}$. No mutation occurs at those loci (the fraction that fixes stays very low in all the simulations). We set the segregational variance to $\sigma^2 = 0.01$ small, so that our analysis in a small variance is a good approximation. Note also that the absolute maximum infinitesimal contribution to the trait of an individual is: $\sigma\sqrt{L} = 2.5 \geq \theta$, and is therefore more than enough to match the difference in the optima.

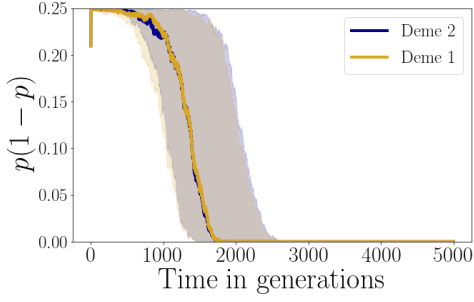
There is an additional locus of interest, which carries the major alleles $+\eta$ or $-\eta$. This locus is also unlinked to all the others and no mutation occurs at this site.

Life cycle. The life cycle involves non-overlapping generations and proceeds as follows:

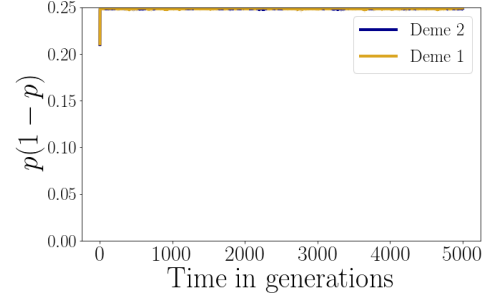
1. *reproduction*: each individual of the meta-population chooses at random one mate within its subpopulation, and their mating produces an offspring.
2. *selection-competition*: each individual faces a selection-competition trial according to its trait ζ and habitat i in which they are currently living. They survive with probability $\min \left[1, \exp(-g(\zeta - \theta_i)^2) \exp\left(1 - \frac{N_i}{K}\right) \right]$ and are removed otherwise.
3. *migration*: at each migration event, within each subpopulation i , a number of migrants is drawn, according to a Poisson probability with parameter $m N_i$ (with a hard cap of N_i , that is the number of individuals currently in the subpopulation). Migrants are uniformly sampled accordingly within the subpopulation and are moved to the other deme.

Each simulation repeats this life cycle, first without migration for 100 generations of burn in and next for $N_{\text{gen}} = 5 \times 10^3$ generations with migration.

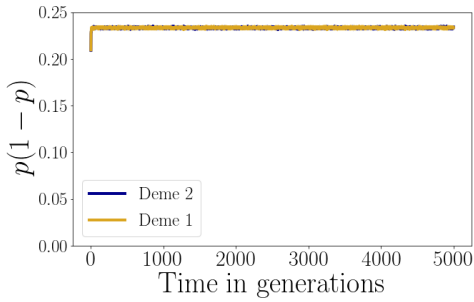
Control case without infinitesimal background. To confirm our simulations, we additionally run an equal number of replicates for each set of parameters without any infinitesimal background ($L = 0$). Only the major alleles are segregating, and this corresponds to the one-locus haploid model. Results shown in the right panel of Fig. 6 are consistent with the one-locus haploid model analysis, that states that the polymorphism at this major locus is stable at all level of selection.



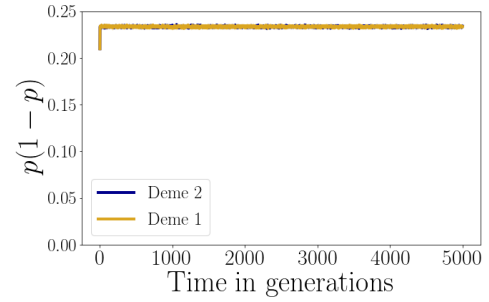
(a) Major locus with infinitesimal background: weak selection ($g = 0.1$). polymorphism at the major locus is lost after some generations (fixation of one allele, loss of the other one).



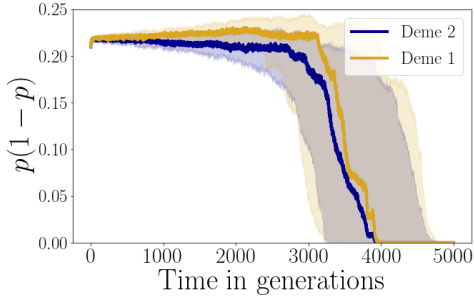
(b) Control case without infinitesimal background (corresponding to the one-locus haploid model): weak selection ($g = 0.1$). polymorphism at the major locus is maintained over the course of all simulations.



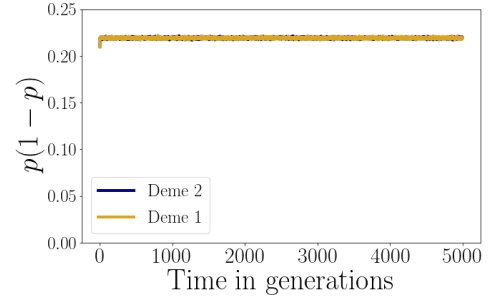
(c) Major locus with infinitesimal background: intermediate selection ($g = 0.5$). polymorphism at the major locus is maintained over the course of all simulations.



(d) Control case without infinitesimal background (corresponding to the one-locus haploid model): intermediate selection ($g = 0.5$). polymorphism at the major locus is maintained over the course of all simulations.



(e) Major locus with infinitesimal background: strong selection ($g = 1$). polymorphism at the major locus is lost after some generations.



(f) Control case without infinitesimal background : strong selection ($g = 1$). polymorphism at the major locus is maintained over the course of all simulations.

Figure 6: **Variance at the major locus across generations, for increasing selection (top to bottom: $g = 0.1, 0.5, 1$) at a fixed rate of migration ($m = 0.3$).** p denotes the local frequency of the major allele A . The left panel is obtained with both a major locus ($\eta = 1/2$) and an infinitesimal background, whereas only the major locus is present in the right panel. For each subfigure, 20 replicates simulations were run per set of parameters, according to the setting explained in Section 5. In each subfigure, the solid line represents the median trajectory and the shaded area indicates the 0.2 and 0.8 quantiles. This figure confirms that polymorphism of the major-effect locus is maintained only when selection is intermediate in strength in presence of a infinitesimal background.

6 Discussion

Contributions. In this work, we present a new model for selection in a heterogeneous environment that combines a major-effect locus with a quantitative genetic background, without assuming that the latter are normally distributed. This model bridges a population genetic model (one-locus haploid model) with a quantitative genetic model recently studied in a heterogeneous environment (Dekens 2020). To do so, it introduces a new reproduction operator, inspired by the infinitesimal model, that encodes the inheritance of a major effect and a quantitative background. The analysis goes deeper than previous studies (Lande 1983), by formally justifying, in a regime of small variance, that the polygenic component of the trait is normally distributed around the major allelic effects. To that effect, we find new convex analysis arguments that leads to a separation of time scales, which allows us to study the stability of the polymorphism at the major locus. We show that this polymorphism, which is maintained at intermediate selection, is subsequently lost when selection increases beyond a certain threshold, a phenomenon qualitatively confirmed by individual-based simulations. The separation of time scales’ point of view offers the interpretation that the infinitesimal background slowly disrupts the fast established symmetrical polymorphism at the major locus. Therefore, this phenomenon cannot be predicted by the one-locus haploid model (without the quantitative background). To our knowledge, this phenomenon has not yet been documented.

Summary of complete analytical outcomes. The analysis performed in Section 4 is centered on the persistence of polymorphism at the major effect locus. As stated in Working assumption 1, the loss of polymorphism by fixation would lead to the dynamics of the quantitative background alone, as covered in Dekens (2020). Hence, Fig. 7 complements Fig. 4 (for $\eta = 0.5$ and varying migration and selection), by displaying both the region of parameters where the system would go to the symmetrical polymorphic equilibrium (in yellow, corresponding to the region where polymorphism is stable), and the region of parameters corresponding to the two types of monomorphic equilibria for a quantitative trait in the regime of small variance described in Dekens (2020).

For bounded selection, there exists a critical threshold in the migration rate under which the polymorphism at the major locus is stable (yellow region) and above which it is lost due to the strong blending effect of migration. In that case, the population trait distribution is concentrated on the trait at the midpoint between the two habitats’ optima, and occupies equally the two habitats. this corresponds to the symmetrical monomorphic equilibrium (see Ronce and Kirkpatrick 2001; Dekens 2020), where the population can be qualified as generalist (green region). One can notice that there exists an interval of selection strengths $g \in [0.7, 1]$ in which the major polymorphism might not be stable for all migration rates under the critical threshold. This phenomenon does not hold for greater major allelic effects (see Fig. 4b, Fig. 4c, Fig. 4d).

For bounded migration rates, and with weak selection, the major polymorphism is unstable, as the diverging selection is too weak compared to the blending migration to maintain differentiation at the major locus (green region). When selection strength increases, the polymorphism at the major locus is first stable (yellow region), but eventually lost above a certain selection strength. The population becomes adapted to one of the two habitats that it mostly inhabits (blue region). This asymmetrical equilibria, highlighted as a source-sink scenario in Ronce and Kirkpatrick (2001), was analytically derived in Dekens (2020).

Extensions to more complex population genetic models. We provide a comprehensive toolbox (Appendix A) at the end of this document, to describe how to apply the method

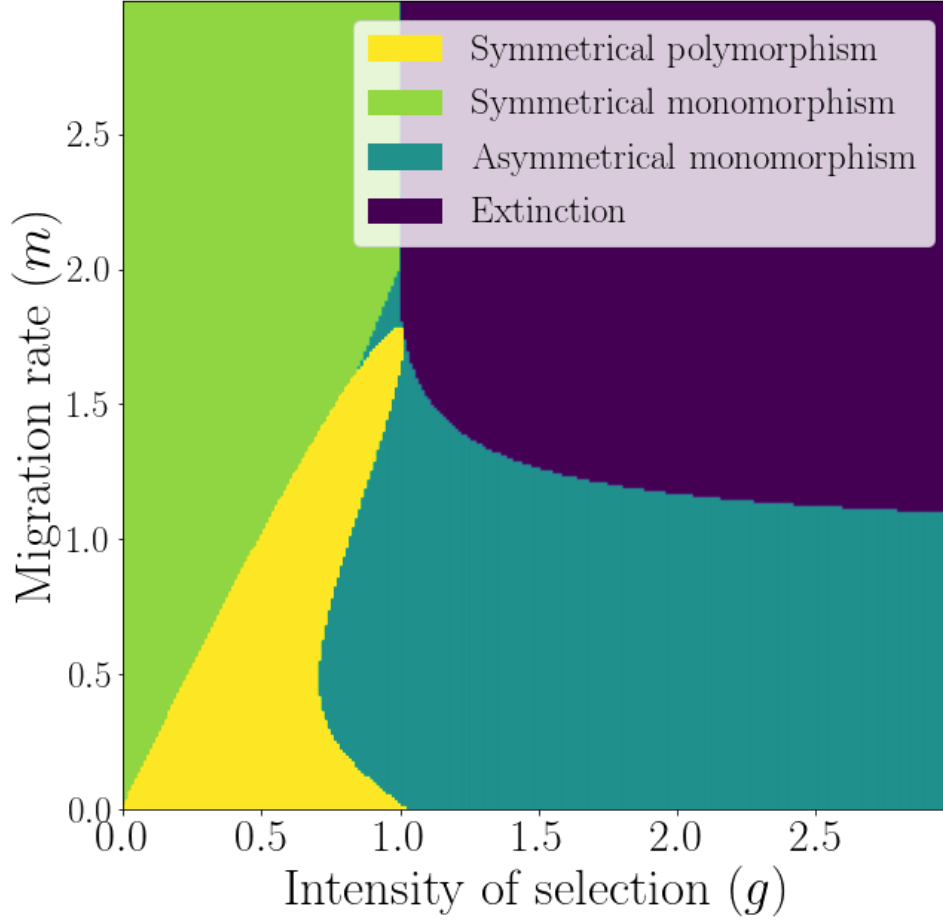


Figure 7: **Summary of the complete analytical outcomes of the model**, for $\eta = 0.5$ and varying migration (y -axis) and selection (x -axis). The figure combines the results obtained in Section 4 on the stability of the symmetrical polymorphic equilibrium with the results of the model of Dekens (2020) (equivalent to this model upon loss of polymorphism). For bounded selection, when migration increases, there is a threshold over which the polymorphism at the major locus is lost due to the blending effect of migration (consistent with Yeaman and Whitlock 2011). The population becomes equally maladapted to both habitats (generalist - symmetrical monomorphism, in the green region). For this specific major allelic effect $\eta = 0.5$, there exists additionally an interval of selection strength ($\approx [0.7 - 1]$) for which the major polymorphism is not stable at migration rates below the critical threshold. This phenomenon does not seem to hold when the allelic effect is larger (see Fig. 4b). For bounded migration (below the threshold rate over which the strong migration blending hampers the major polymorphism), when selection strength increases, the polymorphism at the major allele (yellow region) is lost, and the population becomes adapted to one of the two habitats (specialist - asymmetrical monomorphism, in the blue region). As this figure is obtained in the small segregational variance regime (which should remain smaller than the other parameters of the system for the analysis to be valid), we warn that the outcomes displayed in the vicinity of the x -axis (very small migration rates) might not correspond to the limit when the migration rate is 0 (no migration).

more broadly. In particular, the toolbox is meant to indicate how to extend the method to more complex population genetic models by adding a quantitative background. It relies on [Proposition B.1](#), and we detail the hypotheses that the population genetic models must satisfy in order to use it (see [Appendix B](#) for details and examples).

Further prospects. The loss of the polymorphism at the major locus at strong selection levels in heterogeneous environment, where one might think that it is most favoured, illustrates the value of our method. However, a natural question would be: does this phenomenon hold if the major alleles are allowed to accumulate mutations? [Figure 4](#) for example suggests that polymorphism at the major-effect locus would persist over a wider range of parameters if the alleles at the major-effect locus evolve to match the difference in optima. This possibility was indicated by the numerical findings of Yeaman and Whitlock ([2011](#)), who found the emergence of tightly linked clusters of major loci underlying local adaptation for intermediate migration rates. To study this phenomenon, a more complex model is required, which will be the prospect of a future work.

Acknowledgements

The authors thank Sepideh Mirrahimi, Florence Débarre and Barbara Neto-Bradley for enlightening conversations. This project has received funding from the European Research Council (ERC) under the European Union’s Horizon 2020 research and innovation programme (grant agreement No 639638).

References

- [BA11] R. Bürger and A. Akerman. “The effects of linkage and gene flow on local adaptation: A two-locus continent-island model”. In: *Theor. Popul. Biol.* 80.4 (Dec. 2011), pp. 272–288. ISSN: 00405809. DOI: [10.1016/j.tpb.2011.07.002](#).
- [BEV17] N. H. Barton, A. M. Etheridge, and A. Véber. “The infinitesimal model: Definition, derivation, and implications”. In: *Theor. Popul. Biol.* 118 (Dec. 2017), pp. 50–73. ISSN: 00405809. DOI: [10.1016/j.tpb.2017.06.001](#).
- [BMP09] G. Barles, S. Mirrahimi, and B. Perthame. “Concentration in Lotka-Volterra Parabolic or Integral Equations: A General Convergence Result”. In: *Methods and Applications of Analysis* 16.3 (2009), pp. 321–340. ISSN: 10732772, 19450001. DOI: [10.4310/MAA.2009.v16.n3.a4](#).
- [Bou+] E. Bouin et al. “Equilibria of quantitative genetics models beyond the Gaussian approximation I: Maladaptation to a changing environment”. In: (), p. 41.
- [Bul71] M. G. Bulmer. “The Effect of Selection on Genetic Variability”. In: *Am. Nat.* 105.943 (1971), pp. 201–211.
- [CGP19] V. Calvez, J. Garnier, and F. Patout. “Asymptotic analysis of a quantitative genetics model with nonlinear integral operator”. In: *J. de l’École Polytechnique* 6 (2019), pp. 537–579. ISSN: 2270-518X. DOI: [10.5802/jep.100](#).
- [CH08] Luis-Miguel Chevin and Frédéric Hospital. “Selective Sweep at a Quantitative Trait Locus in the Presence of Background Genetic Variation”. In: *Genetics* 180.3 (Nov. 2008), pp. 1645–1660. ISSN: 1943-2631. DOI: [10.1534/genetics.108.093351](#).

- [Dek20] Léonard Dekens. *Evolutionary dynamics of complex traits in sexual populations in a strongly heterogeneous environment: how normal?* 2020. arXiv: [2012.10115](https://arxiv.org/abs/2012.10115) [q-bio.PE].
- [Die+05] O. Diekmann et al. “The dynamics of adaptation: An illuminating example and a Hamilton-Jacobi approach”. In: *Theor. Popul. Biol.* 67.4 (June 2005), pp. 257–271. ISSN: 0040-5809. DOI: [10.1016/j.tpb.2004.12.003](https://doi.org/10.1016/j.tpb.2004.12.003).
- [Dud+07] J. W. Dudley et al. “Genetic Analysis of Corn Kernel Chemical Composition in the Random Mated 7 Generation of the Cross of Generations 70 of IHP × ILP”. In: *Crop Science* 47.1 (2007), pp. 45–57. DOI: <https://doi.org/10.2135/cropsci2006.03.0207>. eprint: <https://access.onlinelibrary.wiley.com/doi/pdf/10.2135/cropsci2006.03.0207>. URL: <https://access.onlinelibrary.wiley.com/doi/abs/10.2135/cropsci2006.03.0207>.
- [Fis19] R. A. Fisher. “The Correlation between Relatives on the Supposition of Mendelian Inheritance.” In: *Transactions of the Royal Society of Edinburgh* 52.2 (1919), pp. 399–433. DOI: [10.1017/S0080456800012163](https://doi.org/10.1017/S0080456800012163).
- [GB14] Ludwig Geroldinger and Reinhard Bürger. “A two-locus model of spatially varying stabilizing or directional selection on a quantitative trait”. In: *Theoretical Population Biology* 94 (June 2014), pp. 10–41. ISSN: 00405809. DOI: [10.1016/j.tpb.2014.03.002](https://doi.org/10.1016/j.tpb.2014.03.002).
- [GT00] Francis R. Groeters and Bruce E. Tabashnik. “Roles of Selection Intensity, Major Genes, and Minor Genes in Evolution of Insecticide Resistance”. In: *Journal of Economic Entomology* 93.6 (Dec. 2000), pp. 1580–1587. ISSN: 00220493, 00220493. DOI: [10.1603/0022-0493-93.6.1580](https://doi.org/10.1603/0022-0493-93.6.1580).
- [HDT01] A. P. Hendry, T. Day, and E. B. Taylor. “POPULATION MIXING AND THE ADAPTIVE DIVERGENCE OF QUANTITATIVE TRAITS IN DISCRETE POPULATIONS: A THEORETICAL FRAMEWORK FOR EMPIRICAL TESTS”. In: *Evolution* 55.3 (Mar. 2001), pp. 459–466. ISSN: 00143820. DOI: [10.1111/j.0014-3820.2001.tb00780.x](https://doi.org/10.1111/j.0014-3820.2001.tb00780.x).
- [HM19] Benjamin C Haller and Philipp W Messer. “SLiM 3: Forward Genetic Simulations Beyond the Wright–Fisher Model”. In: *Molecular Biology and Evolution* 36.3 (Jan. 2019), pp. 632–637. ISSN: 0737-4038. DOI: [10.1093/molbev/msy228](https://doi.org/10.1093/molbev/msy228). eprint: <https://academic.oup.com/mbe/article-pdf/36/3/632/27980602/msy228.pdf>. URL: <https://doi.org/10.1093/molbev/msy228>.
- [HPH19] Ilse Höllinger, Pleuni S. Pennings, and Joachim Hermisson. “Polygenic adaptation: From sweeps to subtle frequency shifts”. In: *PLOS Genetics* 15.3 (Mar. 2019). Ed. by Justin C. Fay, e1008035. ISSN: 1553-7404. DOI: [10.1371/journal.pgen.1008035](https://doi.org/10.1371/journal.pgen.1008035).
- [JS17] Kavita Jain and Wolfgang Stephan. “Rapid Adaptation of a Polygenic Trait After a Sudden Environmental Shift”. In: *Genetics* 206.1 (May 2017), pp. 389–406. ISSN: 1943-2631. DOI: [10.1534/genetics.116.196972](https://doi.org/10.1534/genetics.116.196972).
- [Lan78] K. Lange. “Central limit theorems of pedigrees”. In: *J. Math. Biol.* 6.1 (June 1978), pp. 59–66. ISSN: 0303-6812, 1432-1416. DOI: [10.1007/BF02478517](https://doi.org/10.1007/BF02478517).
- [Lan83] Russell Lande. “The response to selection on major and minor mutations affecting a metrical trait”. In: *Heredity* 50.1 (Feb. 1983), pp. 47–65. ISSN: 0018-067X, 1365-2540. DOI: [10.1038/hdy.1983.6](https://doi.org/10.1038/hdy.1983.6).

- [Lau+04] Cathy C Laurie et al. “The Genetic Architecture of Response to Long-Term Artificial Selection for Oil Concentration in the Maize Kernel”. In: *Genetics* 168.4 (Dec. 2004), pp. 2141–2155. ISSN: 1943-2631. DOI: [10.1534/genetics.104.029686](https://doi.org/10.1534/genetics.104.029686).
- [LL54] J. J. Levin and N. Levinson. “Singular Perturbations of Non-linear Systems of Differential Equations and an Associated Boundary Layer Equation”. In: *J. of Rational Mechanics and Analysis* 3 (1954), pp. 247–270. ISSN: 19435282, 19435290. URL: <http://www.jstor.org/stable/24900288>.
- [Lyt97] K. A. Lythgoe. “Consequences of gene flow in spatially structured populations”. In: *Genetical Research* 69.1 (Feb. 1997), pp. 49–60. ISSN: 00166723. DOI: [10.1017/S0016672397002644](https://doi.org/10.1017/S0016672397002644).
- [MB94] John A. McKenzie and Philip Batterham. “The genetic, molecular and phenotypic consequences of selection for insecticide resistance”. In: *Trends in Ecology & Evolution* 9.5 (1994), pp. 166–169. ISSN: 0169-5347. DOI: [https://doi.org/10.1016/0169-5347\(94\)90079-5](https://doi.org/10.1016/0169-5347(94)90079-5). URL: <https://www.sciencedirect.com/science/article/pii/0169534794900795>.
- [MG20] S. Mirrahimi and S. Gandon. “Evolution of Specialization in Heterogeneous Environments: Equilibrium Between Selection, Mutation and Migration”. In: *Genetics* 214.2 (2020), pp. 479–491. ISSN: 0016-6731. DOI: [10.1534/genetics.119.302868](https://doi.org/10.1534/genetics.119.302868).
- [Mir17] S. Mirrahimi. “A Hamilton-Jacobi approach to characterize the evolutionary equilibria in heterogeneous environments”. In: *Math. Models Methods Appl. Sci.* 27.13 (Dec. 2017), pp. 2425–2460. ISSN: 0218-2025. DOI: [10.1142/s0218202517500488](https://doi.org/10.1142/s0218202517500488).
- [NL01] T. Nagylaki and Y. Lou. “Patterns of Multiallelic Polymorphism Maintained by Migration and Selection”. In: *Theor. Popul. Biol.* 59.4 (June 2001), pp. 297–313. ISSN: 00405809. DOI: [10.1006/tpbi.2001.1526](https://doi.org/10.1006/tpbi.2001.1526).
- [Pat20] Patout. *The Cauchy problem for the infinitesimal model in the regime of small variance*. 2020. arXiv: [2001.04682](https://arxiv.org/abs/2001.04682) [math.AP].
- [PB08] B. Perthame and G. Barles. “Dirac concentrations in Lotka-Volterra parabolic PDEs”. In: *Indiana University Mathematics Journal* 57.7 (2008), pp. 3275–3302. ISSN: 0022-2518. DOI: [10.1512/iumj.2008.57.3398](https://doi.org/10.1512/iumj.2008.57.3398).
- [RK01] O. Ronce and M. Kirkpatrick. “WHEN SOURCES BECOME SINKS: MIGRATIONAL MELTDOWN IN HETEROGENEOUS HABITATS”. In: *Evolution* 55.8 (Aug. 2001), pp. 1520–1531. ISSN: 0014-3820. DOI: [10.1111/j.0014-3820.2001.tb00672.x](https://doi.org/10.1111/j.0014-3820.2001.tb00672.x).
- [Sla05] Jon Slate. “INVITED REVIEW: Quantitative trait locus mapping in natural populations: progress, caveats and future directions”. In: *Molecular Ecology* 14.2 (2005), pp. 363–379. ISSN: 1365-294X. DOI: [10.1111/j.1365-294X.2004.02378.x](https://doi.org/10.1111/j.1365-294X.2004.02378.x).
- [SSB21] Enikő Szép, Himani Sachdeva, and N. H. Barton. “Polygenic local adaptation in metapopulations: A stochastic eco-evolutionary model”. In: *Evolution* 75.5 (2021), pp. 1030–1045. DOI: <https://doi.org/10.1111/evo.14210>. eprint: <https://onlinelibrary.wiley.com/doi/pdf/10.1111/evo.14210>. URL: <https://onlinelibrary.wiley.com/doi/abs/10.1111/evo.14210>.
- [VB14] Harold de Vladar and Nick Barton. “Stability and Response of Polygenic Traits to Stabilizing Selection and Mutation”. In: *Genetics* 197.2 (June 2014), pp. 749–767. ISSN: 1943-2631. DOI: [10.1534/genetics.113.159111](https://doi.org/10.1534/genetics.113.159111).

- [WL18] B. Walsh and M. Lynch. *Evolution and Selection of Quantitative Traits*. OUP Oxford, 2018. ISBN: 978-0-19-256664-5. URL: <https://books.google.co.uk/books?id=L2liDwAAQBAJ>.
- [YO11] S. Yeaman and S. P. Otto. “ESTABLISHMENT AND MAINTENANCE OF ADAPTIVE GENETIC DIVERGENCE UNDER MIGRATION, SELECTION, AND DRIFT”. In: *Evolution* 65.7 (July 2011), pp. 2123–2129. ISSN: 00143820. DOI: [10.1111/j.1558-5646.2011.01277.x](https://doi.org/10.1111/j.1558-5646.2011.01277.x).
- [YW11] S. Yeaman and M. C. Whitlock. “THE GENETIC ARCHITECTURE OF ADAPTATION UNDER MIGRATION-SELECTION BALANCE: THE GENETIC ARCHITECTURE OF LOCAL ADAPTATION”. In: *Evolution* 65.7 (July 2011), pp. 1897–1911. ISSN: 00143820. DOI: [10.1111/j.1558-5646.2011.01269.x](https://doi.org/10.1111/j.1558-5646.2011.01269.x).

A Toolbox: How to study the interplay between a quantitative background and a finite number of major loci.

The aim is to study the interplay between a quantitative background and a finite number of major loci.

We start with a population genetic model. Let us consider I different genotypes $\mathcal{A}^{(i)}$ which have genotypic effects on the phenotype $a^{(i)}$ (we use the index i to indicate genotypes). For our method to be applied, the genotypes should verify two hypotheses H1 and H2 described in Appendix B. The metapopulation lives in a heterogeneous environment of K patches (we use the index k to indicate location). We denote the population of patch k carrying genotype i by $N_k^{(i)}$. Let us denote the system of equations that describes the dynamics of the genotypic local population sizes: $\frac{d\bar{N}}{dT} = \tilde{G}_{\bar{a}}(\bar{N}(T))$ and of a viable stable equilibrium \bar{N}^* . *We recall that \bar{N}^* is an equilibrium of the system if $\tilde{G}_{\bar{a}}(\bar{N}^*) = 0$. This equilibrium is viable if all the population sizes are non-negative, and at least one is positive. Its local stability is determined by standard linear analysis (sign of the real parts of the eigenvalues of the system's Jacobian).*

Let us modify the previous population genetic framework to include the effect of a quantitative background on the trait, generically denoted z . While previously, all individuals carrying the same genotype $\mathcal{A}^{(i)}$ shared the same phenotype, now their phenotypes can differ due to the quantitative background they present. Consequently, among individuals of the same patch k carrying the same major genotype $\mathcal{A}^{(i)}$, we distinguish those sharing the same quantitative background z , and denote their number $n_k^{(i)}(z)$:

$$\begin{aligned}\mathcal{A}^{(i)} &\rightsquigarrow (\mathcal{A}^{(i)}, z) \\ a^{(i)} &\rightsquigarrow a^{(i)} + z \\ N_k^{(i)} &\rightsquigarrow n_k^{(i)}(z).\end{aligned}$$

The PDE system that we obtain on the trait distributions $n_k^{(i)}$ is not easily analysed. That is why we provide a five steps plan in order to guide the analysis when the diversity introduced by the segregation of the quantitative component of the trait is small compared to the variance generated by the major loci (H6 - regime of small variance):

1. first, we operate a scaling of time according to the regime of small variance. It anticipates on the separation of time scales such that the major allelic frequencies change rapidly, followed by the slow changes of the quantitative components (see step 3).
2. in this regime of small variance, we can justify the Gaussian approximation of the local genotypic distributions $n_k^{(i)}$ centered at the same mean and the same variance ε^2 , thanks to Proposition B.1, as soon as the assumptions (H1) and (H2) are satisfied (see Appendix B) and every genotypic population mates with themselves and every other genotypic population (H3) (the latter excludes models that differentiate sexes). This guides the intuition of which change of variables to perform in order to get a system separating time scales explicitly (see Step 3). We emphasize that Proposition B.1 is crucial to be able to apply this method.
3. From the PDE system on the distributions $n_k^{(i)}$, we can deduce the ODE system of their moments. Since we have justified the Gaussian approximation for all local genotypic distributions $n_k^{(i)}$, the new system is closed in the regime of small variance $\varepsilon^2 \ll 1$,

and only involves the dynamics of the genotypic local sizes of populations $N_k^{(i)}$ and the genotypic local mean quantitative components $z_k^{(i)}$.

4. This step aims at obtaining a system that explicitly separates time scales, in order to ultimately reduce the complexity of the analysis. It requires a technical change of variables, which is guided by the formal analysis of the step 1 (mean quantitative components roughly the same within patches), and the intuition that migration has a strong blending effect between patches in the small variance regime (which would result in the mean quantitative components roughly being equal between patches). These considerations bring the following new variables replacing the genotypic local mean quantitative component $z_k^{(i)}$:

- ◊ for each genotype $1 \leq i \leq I$, $\delta_{k,\varepsilon}^{(i)}$ is the difference in the mean quantitative component of the genotypic population i between the patch $k + 1$ and patch k , $1 \leq k \leq K - 1$. Dividing by ε^2 comes from the intuition given above.
- ◊ for each genotype $1 \leq i \leq I - 1$, $\delta_\varepsilon^{(i)}$ is the difference between the mean quantitative component averaged across patches of genotypic population $i + 1$ and i . Dividing by ε^2 comes from the intuition given in Step 1.
- ◊ Z_ε is the overall mean quantitative component across patches and major genotypes. It is the slow evolving variable.

Rewriting the dynamics of the genotypic local population sizes \bar{N}_ε along these new variables $\bar{\delta}_\varepsilon$ and Z_ε delivers a system in which all the differential equations are multiplied by ε^2 (fast dynamics of \bar{N}_ε and $\bar{\delta}_\varepsilon$) except the one governing the dynamics of Z_ε (slow dynamics).

To finally complete the separation of time scales and obtain the limit system by letting ε^2 vanish, it is sufficient to show that at each value Z of the slow variable, the fast time-scale equilibria $(\bar{N}, \bar{\delta})$ are stable, for example by using the Routh Hurwitz criterion for linear analysis on the Jacobian $\text{Jac}_{\mathcal{G}_a}(\bar{N}, \bar{\delta})$.

5. The last step to determine the stability of the global equilibria of the full system of the genotypic population with the influence of the quantitative background $(\bar{N}^*, \bar{\delta}^*, Z^*)$, consists in applying the formula given in the last box (see the next page).

Toolbox: How to study the interplay between a quantitative background and a finite number of major loci dynamics.

Population genetic model

The stadium:

K patches P_k ($1 \leq k \leq K$)

Pop. gen. model:

$$\frac{d\bar{N}}{dT} = \bar{G}_{\bar{a}}(\bar{N}(T))$$

The teams:

I different genotypes $\mathcal{A}^{(i)}$ ($1 \leq i \leq I$)

Vector of genotypic effects on phenotype: $\bar{a} = (a^{(1)}, \dots, a^{(I)})$

Matrix of local genotypic population sizes: $\bar{N} = (N_k^{(i)})$

Pop gen. analysis:

- (i) Viable equilibria: $G_{\bar{a}}(\bar{N}^*) = 0$ and $\bar{N}^* > \bar{0}$.
- (ii) Stability: eigenvalues of $\text{Jac}_{G_{\bar{a}}}(\bar{N}^*)$ in open left plane.

Hybrid model combining population and quantitative genetics

The new players:

- (i) Quantitative background z
- (ii) Individuals carrying genotype i and a quantitative background z have a phenotype $z + a^{(i)}$.
- (iii) Distribution in patch k : $n_k^{(i)}(z)$

Work hypothesis:

- H1 - H2 (reflexivity and irreducible graph - see App.B)
- H3 every genotypic population reproduces with themselves and every other in the same patch
- H4 inheritance of the quantitative background in accordance with the infinitesimal model with segregational variance σ^2 .
- H5 the quantitative background is unlinked to $\mathcal{A}^{(i)}$
- H6 $\sigma^2 \ll \min |a^{(i)}|^2$: small variance regime.

Steps to apply the hybrid analysis

0) Scaling of time $t := \varepsilon^2 T$

($\varepsilon^2 := \frac{\sigma^2}{\min |a^{(i)}|^2} \ll 1 \rightsquigarrow$ few diversity via inf. model of reproduction)

1) Formal analysis (justify Gaussian distribution - Proposition B.1):

- (i) $n_{k,\varepsilon}^{(i)}(z) \approx N_{k,\varepsilon}^{(i)} \times \text{Gauss}(z_{k,\varepsilon}^{(i)}, \varepsilon^2)$
- (ii) $z_{k,\varepsilon}^{(i)} \approx z_{k,\varepsilon}^{(j)}$

2) ODE system of moments ($\bar{z}_\varepsilon := (z_{k,\varepsilon}^{(i)})$):

$$\begin{cases} \varepsilon^2 \frac{d\bar{N}_\varepsilon}{dt} = G_{\bar{a}}(\bar{N}_\varepsilon(t), \bar{z}_\varepsilon(t)), \\ \varepsilon^2 \frac{d\bar{z}_\varepsilon}{dt} = F_{\bar{a}}(\bar{N}_\varepsilon(t), \bar{z}_\varepsilon(t)). \end{cases}$$

3) Slow-fast analysis:

- (i) Change in variables: $\delta_{k,\varepsilon}^{(i)} = \frac{z_{k+1,\varepsilon}^{(i)} - z_{k,\varepsilon}^{(i)}}{2\varepsilon^2} [I(K-1)]$;
 $\delta_\varepsilon^{(i)} = \frac{\sum_k z_{k,\varepsilon}^{(i+1)} - z_{k,\varepsilon}^{(i)}}{2K\varepsilon^2} [(I-1)]$; $Z_\varepsilon = \frac{\sum_{k,i} z_{k,\varepsilon}^{(i)}}{K \times I}$
- (ii) Slow-fast system:

$$\begin{cases} \varepsilon^2 \frac{d[\bar{N}_\varepsilon, \bar{\delta}_\varepsilon]}{dt} = \mathcal{G}_{\bar{a}}(\bar{N}_\varepsilon(t), \bar{\delta}_\varepsilon(t), Z_\varepsilon), \\ \frac{dZ_\varepsilon}{dt} = \mathcal{F}_{\bar{a}}(Z_\varepsilon, \bar{N}_\varepsilon, \bar{\delta}_\varepsilon). \end{cases}$$

- (iii) Separation of time scales (via stability of zeros of $\mathcal{G}_{\bar{a}}$ by Routh-Hurwitz criterion on $\text{Jac}_{\mathcal{G}_{\bar{a}}}(\bar{N}, \bar{\delta})$)

$$\begin{cases} 0 = \mathcal{G}_{\bar{a}}(\bar{N}, \bar{\delta}, Z), \\ \frac{dZ}{dt} = \mathcal{F}_{\bar{a}}(Z, \bar{N}, \bar{\delta}). \end{cases}$$

4) Analysis of the limit system:

- (i) Viable equilibria: $\mathcal{G}_{\bar{a}}(\bar{N}^*, \bar{\delta}^*, Z^*) = \mathcal{F}_{\bar{a}}(Z^*, \bar{N}^*, \bar{\delta}^*) = 0$, $\bar{N}^* > 0$
- (ii) Stability: $\nabla_{\bar{N}, \bar{\delta}} \mathcal{F}_{\bar{a}} \cdot \left(\left[\text{Jac}_{\mathcal{G}_{\bar{a}}}(\bar{N}, \bar{\delta}) \right]^{-1} \partial_Z \mathcal{G}_{\bar{a}} \right) \Big|_{Z^*, \bar{N}^*, \bar{\delta}^*} > 0$.

B Generalization of Proposition 2.1 for more complex genotypes.

To state a generalization of Proposition 2.1, we first need to specify the targeted scope of population genetic models. Let us consider I different genotypes $\mathcal{A}^{(i)}$ that satisfies the following hypotheses relating to how they interact with each other regarding the genotypes of their offspring:

H1 Reflexivity: For all $i \in (1, I)$, the offspring of two parents with the same genotype $\mathcal{A}^{(i)}$ has a positive probability to be of genotype $\mathcal{A}^{(i)}$.

H1 is a natural hypothesis when considering either haploid or diploid populations, even with non-Mendelian processes (genetic linkage/recombination, gene drives), provided that they are not too extreme (lowering the probability of inheriting a certain genotype is fine as long as it does not cancel it). The second hypothesis is more conveniently apprehendable by considering the graph \mathcal{G} whose nodes are the genotypes $\mathcal{A}^{(i)}$. A vertex links two nodes $\mathcal{A}^{(i)}$ and $\mathcal{A}^{(j)}$ if and only if there exists a positive probability that their offspring has genotype $\mathcal{A}^{(i)}$ or $\mathcal{A}^{(j)}$.

H2 Irreducible graph: For all $(i, j) \in (1, I)^2$, there exists a path of vertices of \mathcal{G} connecting $\mathcal{A}^{(i)}$ and $\mathcal{A}^{(j)}$.

This last hypothesis is satisfied by any haploid models, regardless of how many loci are considered, because an offspring can inherit all their alleles from only one parent. Consequently, in that case, every node of the graph is connected to every other. In diploid models, where an offspring can have a different genotype from both its parents, which vertices of the graph \mathcal{G} exist is not clear. However, for example, we can show that the graph corresponding to a diploid model, with L loci and two alleles at each loci, is connected according to **H2**. Indeed, each genotype is directly connected to any other that differs from it from just one allele at one locus. Nevertheless, the interest of **H2** is that it is very easy to verify whether it is satisfied given any particular model.

To state the proposition that generalizes (Proposition 2.1), we first need to define the index set of couples that can yield an offspring with a particular genotype. For $i \leq I$, we denote it by $C^{(i)}$, where $(j, k) \in C^{(i)}$ if and only if parents with genotypes $\mathcal{A}^{(j)}$ and $\mathcal{A}^{(k)}$ can produce an offspring with genotype $\mathcal{A}^{(i)}$. The following proposition characterizes the genotypic functions $u^{\mathcal{A}^{(i)}}$ that respect the following constraints analogous to **C**

$$\forall i \leq I, \quad \forall z \in \mathbb{R}, \quad \max_{(j,k) \in C^{(i)}} \left[\sup_{z_1, z_2} u^{\mathcal{A}^{(i)}}(z) - \left(z - \frac{z_1 + z_2}{2} \right)^2 - u^{\mathcal{A}^{(j)}}(z_1) - u^{\mathcal{A}^{(k)}}(z_2) \right] = 0. \quad (\text{C}')$$

Proposition B.1. *Suppose that **H1** and **H2** are satisfied. For $i \in I$, we consider $u^{\mathcal{A}^{(i)}}$ a real valued non-negative function whose zero set is non-empty and of measure 0 (for example, is finite). If $\{u^{\mathcal{A}^{(i)}}, i \leq I\}$ respects (C'), then there exists $z^* \in \mathbb{R}$ such that for all $i \leq I$:*

$$\forall z \in \mathbb{R}, \quad u^{\mathcal{A}^{(i)}}(z) = \frac{(z - z^*)^2}{2}.$$

Proof.

1) $u^{\mathcal{A}^{(i)}}$ **cancels only once.** Let us fix $i \leq I$. Let us suppose that $u^{\mathcal{A}^{(i)}}$ has two zeros $z_1^* \neq z_2^*$. **H1** implies that $(i, i) \in C^{(i)}$. Then, we deduce from (C') that:

$$u^{\mathcal{A}^{(i)}}(z) \leq \inf_{z_1, z_2} \left(z - \frac{z_1 + z_2}{2} \right)^2 + u^{\mathcal{A}^{(i)}}(z_1) + u^{\mathcal{A}^{(i)}}(z_2).$$

In particular, for $z = \frac{z_1^* + z_2^*}{2}$, $z_1 = z_1^*$, $z_2 = z_2^*$, we obtain

$$u^{\mathcal{A}^{(i)}}\left(\frac{z_1^* + z_2^*}{2}\right) \leq 0. \quad (30)$$

As $u^{\mathcal{A}^{(i)}}$ is non-negative, the midpoint between two zeros of $u^{\mathcal{A}^{(i)}}$ is also a zero of $u^{\mathcal{A}^{(i)}}$. $u^{\mathcal{A}^{(i)}}$ is also continuous (the argument is the same as in [Proposition 2.1](#), therefore, we deduce that $u^{\mathcal{A}^{(i)}}$ cancels on $[z_1^*, z_2^*]$. The latter violates the assumption that $u^{\mathcal{A}^{(i)}}$ has a zero set of measure 0. Because it is also not empty, we get that $u^{\mathcal{A}^{(i)}}$ cancels exactly once, in a point that we denote z_i^* .

2) **The zero of $u^{\mathcal{A}^{(i)}}$ coincides with the zero of $u^{\mathcal{A}^{(j)}}$:** $z_i^* = z_j^*$. First, let us consider the case where $(i, j) \in (1, I)^2$ is such that $\mathcal{A}^{(i)}$ and $\mathcal{A}^{(j)}$ are linked by a vertex in the graph \mathcal{G} . Then, we deduce that $(i, j) \in C^{(i)}$ or $(i, j) \in C^{(j)}$. We can assume the first without loss of generality. Similarly as the first part of the proof, we deduce that

$$u^{\mathcal{A}^{(i)}}(z) \leq \inf_{z_1, z_2} \left(z - \frac{z_1 + z_2}{2} \right)^2 + u^{\mathcal{A}^{(i)}}(z_1) + u^{\mathcal{A}^{(j)}}(z_2).$$

Consequently, the midpoint between z_i^* and z_j^* is a zero of $u^{\mathcal{A}^{(i)}}$, which is necessarily z_i^* , which implies that $z_i^* = z_j^*$.

Let us now show the same for every couple (i, j) not necessarily linked by a vertex in \mathcal{G} . **H2** implies that there exists a path of vertices between $u^{\mathcal{A}^{(i)}}$ and $u^{\mathcal{A}^{(j)}}$. As we showed that for every pair of nodes connected by a vertex, the zeros of their function is the same point, that property also holds for the extremities of the path of vertices, hence $z_i^* = z_j^*$. We denote z^* the common zero.

3) **Convex Legendre conjugates** $u^{\hat{\mathcal{A}}^{(i)}}(y) = \sup_z (z - z^*)y - u^{\mathcal{A}^{(i)}}(z)$. Similarly as in [Proposition 2.1](#), (C') implies that the convex Legendre conjugate satisfies

$$\forall y \in \mathbb{R}, \quad u^{\hat{\mathcal{A}}^{(i)}}(y) = \frac{y^2}{4} + \max_{(j, k) \in C^{(i)}} \left[u^{\hat{\mathcal{A}}^{(j)}}\left(\frac{y}{2}\right) + u^{\hat{\mathcal{A}}^{(k)}}\left(\frac{y}{2}\right) \right]. \quad (31)$$

Moreover, we obtain classically that:

$$u^{\hat{\mathcal{A}}^{(i)}}(y) \geq (z^* - z^*)y - u^{\mathcal{A}^{(i)}}(z^*) = 0 = u^{\hat{\mathcal{A}}^{(i)}}(0) \quad (32)$$

.

4) $\max_{i \leq I} u^{\hat{\mathcal{A}}^{(i)}} : y \mapsto \frac{y^2}{2}$. We obtain from (31) that:

$$\forall y \in \mathbb{R}, \quad \max_{i \leq I} u^{\hat{\mathcal{A}}^{(i)}}(y) = \frac{y^2}{4} + \max_{i \leq I} \max_{(j, k) \in C^{(i)}} \left[u^{\hat{\mathcal{A}}^{(j)}}\left(\frac{y}{2}\right) + u^{\hat{\mathcal{A}}^{(k)}}\left(\frac{y}{2}\right) \right]. \quad (33)$$

For $y \in \mathbb{R}$, let $i_0 \leq I$ be such that $\max_{i \leq I} u^{\hat{\mathcal{A}}^{(i)}}\left(\frac{y}{2}\right) = u^{\hat{\mathcal{A}}_{i_0}}\left(\frac{y}{2}\right)$. **H1** implies in particular $(i_0, i_0) \in C^{(i_0)}$ and therefore, the maximum of the r.h.s of (33) is reached in $2u^{\hat{\mathcal{A}}_{i_0}}\left(\frac{y}{2}\right)$. Consequently, we deduce that

$$\forall y \in \mathbb{R}, \quad \max_{i \leq I} u^{\hat{\mathcal{A}}^{(i)}}(y) = \frac{y^2}{4} + 2 \max_{i \leq I} u^{\hat{\mathcal{A}}^{(i)}}\left(\frac{y}{2}\right). \quad (34)$$

Moreover, one can notice that

$$\begin{aligned} \forall y \in \mathbb{R}, \quad \max_{i \leq I} u^{\hat{\mathcal{A}}^{(i)}}(y) &= \max_{i \leq I} \max_{z \in \mathbb{R}} (z - z^*)y - u^{\mathcal{A}^{(i)}}(z) \\ &= \max_{z \in \mathbb{R}} (z - z^*)y - \min_{i \leq I} u^{\mathcal{A}^{(i)}}(z) \\ &= \left(\min_{i \leq I} u^{\hat{\mathcal{A}}^{(i)}} \right)(y). \end{aligned}$$

Therefore, $\max_{i \leq I} u^{\hat{\mathcal{A}}^{(i)}}$ is a convex continuous function that has left and right derivative everywhere, in particular in 0. Hence, similarly as in Proposition 2.1, iterating (34) implies first that:

$$\forall y > 0 \quad (\text{resp. } < 0), \quad \max_{i \leq I} u^{\hat{\mathcal{A}}^{(i)}}(y) = \frac{y^2}{2} + \beta y \quad (\text{resp. } \alpha y), \quad (35)$$

where $(\alpha, \beta) = \left(\max_{i \leq I} u^{\hat{\mathcal{A}}^{(i)'}}(0^-), \max_{i \leq I} u^{\hat{\mathcal{A}}^{(i)'}}(0^+) \right)$. From (32), we deduce that the $\alpha \leq 0 \leq \beta$. Since $\max_{i \leq I} u^{\hat{\mathcal{A}}^{(i)}}$ is the convex conjugate of $\min_{i \leq I} u^{\mathcal{A}^{(i)}}$, we deduce that the convex bi-conjugate of $\min_{i \leq I} u^{\mathcal{A}^{(i)}}$ is

$$z \mapsto \begin{cases} \frac{(z - z^* - \alpha)^2}{2} & \text{if } z < z^* + \alpha \\ 0 & \text{if } z^* + \alpha \leq z \leq z^* + \beta \\ \frac{(z - z^* - \beta)^2}{2} & \text{if } z > z^* + \beta. \end{cases} \quad (36)$$

As the convex bi-conjugate of $\min_{i \leq I} u^{\mathcal{A}^{(i)}}$ is the lower convex envelope of $\min_{i \leq I} u^{\mathcal{A}^{(i)}}$, the two of them are equal at the extremal points of its graph, namely for $z = z^* + \alpha$ and $z = z^* + \beta$. We deduce from (36) that

$$\min_{i \leq I} u^{\mathcal{A}^{(i)}}(z^* + \alpha) = \min_{i \leq I} u^{\mathcal{A}^{(i)}}(z^* + \beta) = 0.$$

Since all the $u^{\mathcal{A}^{(i)}}$, $i \leq I$ only cancels for $z = z^*$, we obtain that $\alpha = \beta = 0$ and (35) yields that $\max_{i \leq I} u^{\hat{\mathcal{A}}^{(i)}} : y \mapsto \frac{y^2}{2}$.

5) $\max_{i \leq I} u^{\hat{\mathcal{A}}^{(i)}} = \min_{i \leq I} u^{\hat{\mathcal{A}}^{(i)}}$. First let us state that $\min_{i \leq I} u^{\hat{\mathcal{A}}^{(i)}}$ is continuous as minimum of a finite number of continuous functions and that it is non-negative and reaches its minimum in 0, with $\min_{i \leq I} u^{\hat{\mathcal{A}}^{(i)}}(0) = 0$ (from (32)). Moreover, (31) implies that

$$\forall y \in \mathbb{R}, \quad \min_{i \leq I} u^{\hat{\mathcal{A}}^{(i)}}(y) \leq \frac{y^2}{4} + 2 \max_{i \leq I} u^{\hat{\mathcal{A}}^{(i)}}\left(\frac{y}{2}\right) = \frac{y^2}{2}. \quad (37)$$

Therefore $\min_{i \leq I} u^{\hat{\mathcal{A}}^{(i)}}$ has left and right derivatives in 0, and $\min_{i \leq I} u^{\hat{\mathcal{A}}^{(i)'}}(0^+) = \min_{i \leq I} u^{\hat{\mathcal{A}}^{(i)'}}(0^-) = 0$. Furthermore, (31) also implies that

$$\forall y \in \mathbb{R}, \quad \min_{i \leq I} u^{\hat{\mathcal{A}}^{(i)}}(y) \geq \frac{y^2}{4} + 2 \min_{i \leq I} u^{\hat{\mathcal{A}}^{(i)}}\left(\frac{y}{2}\right).$$

Iterating the last inequality, and knowing that

$$\min_{i \leq I} u^{\hat{\mathcal{A}}^{(i)}}(0) = \min_{i \leq I} u^{\hat{\mathcal{A}}^{(i)'}}(0^+) = \min_{i \leq I} u^{\hat{\mathcal{A}}^{(i)'}}(0^-) = 0,$$

leads to

$$\forall y \in \mathbb{R}, \quad \min_{i \leq I} u^{\hat{\mathcal{A}}^{(i)}}(y) \geq \frac{y^2}{2} = \max_{i \leq I} u^{\hat{\mathcal{A}}^{(i)}}(y).$$

Consequently, we deduce that $\min_{i \leq I} u^{\hat{\mathcal{A}}^{(i)}} = \max_{i \leq I} u^{\hat{\mathcal{A}}^{(i)}}$.

End of proof. The last result implies that

$$\forall i \leq I, \quad \forall y \in \mathbb{R}, \quad u^{\hat{\mathcal{A}}^{(i)}}(y) = \max_{i \leq I} u^{\hat{\mathcal{A}}^{(i)}}(y) = \frac{y^2}{2}.$$

From the latter we compute the bi-conjugates $u^{\hat{\mathcal{A}}^{(i)}} : z \mapsto \frac{(z-z^*)^2}{2}$. Since $z \mapsto \frac{z-z^*}{2}$ is strictly convex and it is the lower convex envelope of $u^{\mathcal{A}^{(i)}}$, we obtain that

$$\forall i \leq I, \quad \forall z \in \mathbb{R}, \quad u^{\mathcal{A}^{(i)}}(z) = \frac{(z-z^*)^2}{2}.$$

□

C Formal justification of the constraints (C) on the main terms u_0^A and u_0^a

We drop the index i indicating the habitat and the time dependence t for this appendix for the sake of simpler notations.

Let us first formally justify that U_0^A and U_0^a are positive almost everywhere and cancelling somewhere. As we are interested in the maintenance of the polymorphism at the major locus, we consider that no major allele has yet fixed. Hence, N_ε^A and N_ε^a need to remain positive and bounded when ε vanishes. Using the Hopf-Cole transforms on n_ε^A and n_ε^a (5) along with the formal Taylor expansions (6) on U_ε^A and U_ε^a leads to

$$N_\varepsilon^A = \int_{\mathbb{R}} n_\varepsilon^A(z') dz' = \int_{\mathbb{R}} \frac{1}{\sqrt{2\pi\varepsilon}} e^{-\frac{U_\varepsilon^A(z')}{\varepsilon^2}} dz' = \int_{\mathbb{R}} \frac{1}{\sqrt{2\pi\varepsilon}} e^{-\frac{u_0^A(z')}{\varepsilon^2}} e^{-u_1^A + \varepsilon^2 v_\varepsilon^A} dz'. \quad (38)$$

If we assume that the residues u_1^A and v_ε^A stay bounded when ε vanishes (as Calvez, Garnier, and Patout (2019) suggests it), then (38) implies that u_0^A must be non-negative for N_ε^A to remain bounded when ε vanishes. For N_ε^A not to vanish asymptotically, u_0^A must cancel. Moreover, for any interval $I \subset \mathbb{R}$, u_0^A cannot cancel on I , or we would have:

$$N_\varepsilon^A > \int_I \frac{1}{\sqrt{2\pi\varepsilon}} e^{\frac{1}{\varepsilon^2}} e^{-u_1^A + \varepsilon^2 v_\varepsilon^A} dz' \rightarrow +\infty.$$

So u_0^A is positive almost everywhere, and cancelling somewhere. The same holds for u_0^a .

Now, for determining the constraints (C), let us notice that if we divide the r.h.s of the first equality of (3) by $n_\varepsilon^A(z)$, the reproduction term $\frac{\mathcal{B}_\varepsilon^A(n_\varepsilon^A, n_\varepsilon^a)(z)}{n_\varepsilon^A(z)}$ has to remain positive and bounded for all $z \in \mathbb{R}$ when ε vanishes for the effect of reproduction to remain well-balanced with selection, migration and competition. We assume henceforth that (6) is the correct ansatz (as suggested by Calvez, Garnier, and Patout 2019). Using the Hopf-Cole transforms on n_ε^A and n_ε^a (5) along with the formal Taylor expansions (6) on U_ε^A and U_ε^a in (4) leads to

$$\begin{aligned} \frac{\mathcal{B}_\varepsilon^A(n_\varepsilon^A, n_\varepsilon^a)(t, z)}{n_\varepsilon^A(z)} &= \frac{\mathcal{B}_\varepsilon^A(n_\varepsilon^A, n_\varepsilon^a)(z)}{\frac{1}{\sqrt{2\pi\varepsilon}} e^{-\frac{u_0^A(z)}{\varepsilon^2}} e^{-u_1^A(z) + \mathcal{O}(\varepsilon^2)}} \\ &= \frac{\sqrt{2}}{N_\varepsilon^A} \times \\ &\quad \left[\int_{\mathbb{R}^2} \exp \left(\frac{1}{\varepsilon^2} \left[u_0^A(z) - \left(z - \frac{z_1 + z_2}{2} \right)^2 - u_0^A(z_1) - u_0^A(z_2) \right] \right) \exp \left(u_1^A(z) - u_1^A(z_1) - u_1^A(z_2) + \mathcal{O}(\varepsilon^2) \right) dz_1 dz_2 \right. \\ &\quad \left. + \int_{\mathbb{R}^2} \exp \left(\frac{1}{\varepsilon^2} \left[u_0^A(z) - \left(z - \frac{z_1 + z_2}{2} \right)^2 - u_0^A(z_1) - u_0^a(z_2) \right] \right) \exp \left(u_1^A(z) - u_1^A(z_1) - u_1^a(z_2) + \mathcal{O}(\varepsilon^2) \right) dz_1 dz_2 \right]. \end{aligned}$$

As N_ε^A remains bounded and does not vanish asymptotically, we need the maximum of the two integrals nor to vanish, nor to diverge to infinity when ε vanishes, for all $z \in \mathbb{R}$. Therefore the maximum of the terms into brackets that are multiplied by $\frac{1}{\varepsilon^2}$ needs to be null for all $z \in \mathbb{R}$:

$$\begin{aligned} \forall z \in \mathbb{R}, \quad \max \left[\sup_{z_1, z_2} u_0^A(z) - \left(z - \frac{z_1 + z_2}{2} \right)^2 - u_0^A(z_1) - u_0^A(z_2), \right. \\ \left. \sup_{z_1, z_2} u_0^A(z) - \left(z - \frac{z_1 + z_2}{2} \right)^2 - u_0^A(z_1) - u_0^a(z_2) \right] = 0, \end{aligned}$$

which is the first constraint of (C). The same holds for $\frac{\mathcal{B}_\varepsilon^a(n_\varepsilon^A, n_\varepsilon^a)(z)}{n_\varepsilon^a(z)}$, which gives the second constraint of (C).